TRIBHUVAN UNIVERSITY
INSTITUTE OF ENGINEERING
PULCHOWK CAMPUS

THESIS NO.: M-389-MSREE-2021-2024

Direct Lightning Impact Assessment in Solar Mini Grid

by

Anup Devkota

A THESIS
SUBMITTED TO THE DEPARTMENT OF MECHANICAL AND AEROSPACE ENGINEERING IN PARTIAL FULFILLMENT OF THE REQUIREMENTS FOR THE DEGREE OF MASTER OF SCIENCE IN RENEWABLE ENERGY ENGINEERING

DEPARTMENT OF MECHANICAL AND AEROSPACE ENGINEERING
LALITPUR, NEPAL

June, 2024

COPYRIGHT

TRIBHUVAN UNIVERSITY

INSTITUTE OF ENGINEERING

PULCHOWK CAMPUS

DEPARTMENT OF MECHANICAL AND AEROSPACE ENGINEERING

The undersigned certify that they have read, and recommended to the Institute of Engineering for acceptance, a thesis entitled **"Direct Lightning Impact Assessment in Solar Mini Grid"** submitted by Anup Devkota in partial fulfillment of the requirements for the degree of Master of Science in Renewable Energy Engineering.

Supervisor, Dr. Basanta Kumar Gautam
Associate Professor
Department of Electrical Engineering
IOE, Pulchowk Campus, TU

Supervisor, Laxman Motra
Assistant Professor
Department of Mechanical and Aerospace Engineering
IOE, Pulchowk Campus, TU

External Examiner, Er. Bijay Mahato
Assistant Manager
Nepal Electricity Authority

Tribhuvan University
Institute of Engineering
Department of Mechanical and Aerospace Engineering
Pulchowk Campus

Committee Chairperson, Sudip Bhattrai, PhD
Assistant Professor/Head of Department
Department of Mechanical and Aerospace Engineering
IOE, Pulchowk Campus, TU

Date: June 10, 2024

ABSTRACT

Lightning strikes represent a substantial hazard to the electrical distribution network, causing both physical and insulation damage. These effects extend to renewable energy sources, specifically solar photovoltaic (PV) systems, which are vulnerable to lightning strikes. This thesis seeks to completely assess the direct impact of lightning on off-grid solar power systems, with an emphasis on array components, inverters, and loads in a mini solar power grid. The study focuses on modeling and simulating lightning-induced transients, their propagation, and the responses of PV system components. A thorough research technique is provided, which includes system modelling, lightning impulse production, and coupling simulation. The off-grid system is modelled with the Electromagnetic Transients Program (EMTP) program, which captures the behavior of PV arrays, inverters, loads, and lightning strikes. The modeling results reveal that lightning strikes can result in substantial overvoltage on dead end low voltage sides. These findings emphasize the need of having an adequate lightning protection system (LPS) to reduce potential damage and maintain system resilience. Modeling and simulation approaches can be used to identify potential vulnerabilities and protection strategies. The findings of this study help to better understand the risk of lightning strikes and improve the design of photovoltaic systems, ensuring their safe and reliable operation in the renewable energy industry.

ACKNOWLEDGEMENT

I would like to express my sincere gratitude to Associate Professor Dr. Basanta Kumar Gautam and Assistant Professor Laxman Motra for supervising my thesis work. Without their invaluable advice, this research work would not have been concluded.

My sincere thanks to the Head of Department and all the faculty members of Department of Mechanical and Aerospace Engineering and Electrical Engineering for their relentless effort to smoothly conduct this research program.

Also, I am grateful towards Deputy-Director Dr. Laxman Prasad Ghimire, Engineer Amanul Hak Ansari and Technical Officer Saroj Bahadur Karki from AEPC for providing me with valuable guidance. Thanks to my seniors Mr. Nasib Khadka, Mr. Pradip Khatiwada and Mr. Prasis Poudel for their amicable support and assistance in times of difficulty.

TABLE OF CONTENTS

LIST OF TABLES

LIST OF FIGURES

LIST OF ACRONYMS

SDG	Sustainable Development Goals
AEPC	Alternative Energy Promotion Centre
CG	Cloud to Ground
GM	Geometric Mean
GFD	Ground Flash Density
NLDN	National Lightning Detection Network
CFO	Critical Flashover Voltage
GSD	Ground Stroke Density
GSPD	Ground Strike Point Density
SW	Shield Wire
SA	Surge Arrester
DDC	Direct Discharge Crossing
CP	Constant Parameter
FD	Frequency-Dependent
ULM	Universal Line Model
NGLA	Non-Gap Lightning Arrester
EGLA	External Gap Lightning Arrester
GIS	Global Horizontal Irradiation
SLD	Single Line Diagram
CIGRE	Council on Large Electric Systems
IEEE	Institute of Electrical and Electronics Engineers
MDPI	Multidisciplinary Digital Publishing Institute
EPSR	Electric Power Systems Research

CHAPTER ONE: INTRODUCTION

1.1 Background

Renewable energy technology is a rapidly developing sector with the potential for substantial technical improvements in the future. The extensive promotion and expansion of renewable energy services have a significant positive impact on the quality of life of people in rural and remote areas of Nepal. Decentralized renewable energy sources remain the most accessible and cost-effective energy solution in such areas. They improve power dependability, diversify energy sources, provide energy security, minimize dependency on fossil fuels, and aid in reducing carbon emissions. Nepal has pledged to reach the Sustainable Development Goals (SDG)-7 target of providing affordable, dependable, sustainable and modern energy to all by 2030. As a result, Nepal has set an aim of providing electricity power to 99% of households by 2030.

Nepal has an enormous opportunity to gather energy using a solar photovoltaic system since it receives lots of sunlight, with an average solar radiation of 4.4 kWh/m^2 to 5.5 kWh/m^2 and around 300 bright days per year (Solargis, 2019). Off-grid solar PV systems can be an excellent choice for both basic and advanced energy requirements. Basic demands include lights, mobile charging, and so forth, but advanced needs include offsetting industry-level grid power through comprehensive cost-benefit analysis. Solar PV systems offer various advantages, particularly when compared to conventional fossil fuels. Solar energy has several advantages, including clean energy, little noise, cheap maintenance costs, and a wide range of uses [1]. However, solar PV systems are typically installed and exposed on rooftops or in outdoor locations, the possibility of such a system being struck by lightning is quite high, particularly in lightning-prone areas.

Lightning is one of the most critical threats in electricity distribution networks. Lightning return strokes have two significant impacts: physical damage and insulation failure [2]. Understanding the direct impact of lightning on a solar PV system (including array, inverters, and load) is critical for maintaining its safety and reliability within a solar mini grid. The assessment of these impacts includes a thorough examination of lightning characteristics, inverter vulnerabilities, and mitigation methods. It

necessitates a thorough understanding of the behavior of lightning-induced transients, their propagation through the components, and their responses to the transients.

1.2 Problem Statement

Nepal has a diverse topography that includes high mountains, valleys and varying altitudes which influences weather patterns creating conditions that are conductive to lightning. Bay of Bengal plays a crucial role in Nepal's climate. The moist air when encounters the mountainous terrain, forced to rise cooling and condensing, forming clouds and potentially leading to thunderstorms. Lightning is also dangerous in high mountains because it travels shorter distances to reach the ground. In Nepal, 34% of cloud to ground lightning strikes are positively charged [3].

Direct and indirect lightning strokes can cause insulation failures and physical damage to power distribution networks [4]. Lighting dangers to distribution networks include line failure, transformer and arrester failure, wooden pole top fire, insulator penetration, cable degradation and damage to low voltage consumer products[5], [6].

The problem addressed by this thesis is the comprehensive and reliable assessment methods for the impact of lightning on solar mini grid systems. Lightning strikes may cause extensive damage to solar panels, inverters, overhead distribution line and other components, resulting in extended power interruptions and costly repairs. While there are existing methods for lightning protection and mitigation, there is a lack of clear standards for their application in solar mini grids. Therefore, there is a need to develop more effective and efficient assessment methods for lightning impact on solar mini grids and propose best practices for lightning protection and mitigation. The aim of this thesis is to address this problem by investigating different assessment methods, evaluating their effectiveness and reliability and proposing recommendations for lightning protection in solar mini grids.

The inevitable fact that lightning causes monetary losses which includes power interruption and voltage sag for short term and damage/ageing of equipment for long term impact is of great concern to utility providers. So, the solar mini grid system should be designed with appropriate lightning schemes to improve line performance during thunderstorms.

1.3 Objectives

1.3.1 Main Objective

The main objective of this thesis is to assess the lightning impacts on solar mini grid systems to understand the behavior of lightning induced transients.

1.3.2 Specific Objectives

The specific objectives are:

- To develop models that accurately represent behavior and characteristics of solar mini grid systems including distribution network.
- To simulate impulse voltage and currents during lightning strokes and study their impact on the solar mini grid system.
- To identify critical areas susceptible to lightning induced voltage and propose effective protection strategies to enhance system resilience.

1.4 Limitation of Research

This research is based on the load flow circumstances of a 60 kWp Sanagau Solar Mini Grid located in Sinja Rural Municipality-05, Jumla, which is currently being implemented by the Alternative Energy Promotion Centre. As a result, the output may differ based on the type of mini grid. Lightning strikes can vary widely in frequency and intensity, making it difficult to precisely predict or model their effects on other interrelated systems. The study focuses on the loss and terminal voltage parameters to calculate the lightning impact assessment. This thesis assesses the consequences of a small distribution system.

CHAPTER TWO: LITERATURE REVIEW

2.1 Solar Mini Grid

Providing access to electricity to a large section of the rural population in Nepal has traditionally been a challenging exercise. This has been due to difficult geography, poor-socio-economic profile of rural Nepal and moreover by the on-going energy crisis. Among renewable energy technologies, solar mini grid is one of the appropriate and viable options which can contribute to the energy mix as it is comparatively cleaner, cheaper and faster to build. Mini-grid systems that provide grid quality electricity are among the most deployed technologies for providing renewable energy solutions around the world. Nepal has also successfully implemented community electrification schemes based on hydro and solar mini-grid systems in many off-grid locations serving a large population previously devoid of electricity access. Mini grids not only provide clean and affordable lighting solutions but also contribute to the local rural economy by providing opportunities to establish enterprises thereby creating employment opportunities at the local level. In the area where there is no grid connection till the date or where there are no mini/micro hydro plants in Nepal, solar PV based electrification projects can generate electricity efficiently and relatively cheaper.

2.2 Lightning in Overhead Distribution Networks

2.2.1 Lightning and its Parameters

Lightning is caused by a self-propagating leader, which generates a channel for the flow of lightning return stroke current. The leader stream is intermittent in the early strokes, known as the stepped leader, and continuous in later strokes, known as dart leaders. The high potential difference between the leader and ground, typically in megavolts, causes the channel to heat up to 30,000 ºK at 10atm pressure. And it is discovered that a complete leader-return stroke releases energy in the order of 10^9 J; yet only 10^{-2} to 10^2 of total energy reaches the strike site.

Lightning is classified into two categories based on discharge locations: cloud flashes and cloud-to-ground flashes. Cloud flashes account for three-fourths of all global lightning activity. Despite accounting for 25% of the total, cloud to ground (CG) flashes are a major source of worry due to their negative impact on human life [7]. CG can be classified into four types: downward negative, downward positive, upward negative, and upward positive, with downward negative lightning accounting for 90% of all CG

flashes [8]. A negative cloud-to-ground lightning flash typically has 3 to 5 strokes with inter-stroke intervals of ten milliseconds (Geometric Mean, GM=60 ms [9]). Nonetheless, single stroke negative CG flashes occur at a rate ranging from 13% to 19% [10], [11], [12], [13], [14], [15], [16]. The strokes that come following the initial stroke are known as subsequent strokes, and they generally follow the pre-existing channel formed by the first strokes to create a new ground terminal. One-third to one-half of all CG lightning has numerous channel terminations separated by distances ranging from 0.3 to 7.3 km (GM=1.7 km) [17]. Positive lightning is less likely to occur due to its high energy concentration, but it is potentially more destructive. They typically occur during the dispersing stage of an individual thunderstorm, particularly in winter thunderstorms and strong storms. Positive lightning can occasionally be triggered by clouds generated by forest fires. Positive lightning is reportedly more common in altitude regions such as Nepal (35% of total lightning) [3].

2.2.2 Lightning Parameter Estimation

Lightning studies have long been carried out in many parts of the world. For engineering studies, the Ground Flash Density (GFD) and the lightning return stroke current are the most essential parameters.

Ground Flash Density (GFD)

Ground Flash Density (GFD) is one of the important parameters in lightning studies, which is a measure of yearly lightning flashes in a square kilometer area. There are three major techniques to identify the GFD of a particular region: lightning flash counter, lightning location system and satellite-based radiation detectors. With the use of multiple-station systems the lightning locating system is considered the most accurate. The lightning flash counter detects the electric or magnetic field generated from the lightning, which exceeds a certain threshold level and is filtered appropriately. While satellite-based detectors detect overall flashes including cloud pulses and GFD is estimated as one third of the total flash density [4]. GFD can sometimes be roughly estimated from the keraunic level if such an instrumentation setup is unavailable. The GFD from the annual number of thunderstorm days (T_d)/the annual number of thunderstorm hour (T_h) can be estimated using below (2.1) (2.2) [18], [19].

$$Ng=0.04* T_d^{1.25} \quad \text{Eq. 2.1}$$

$$Ng=0.054*T_h^{1.1} \quad \text{Eq. 2.2}$$

Return Stroke Current

This parameter is accurately determined through direct current measurements with the help of instrumented towers. Additionally, with lower accuracy, this parameter can also be indirectly estimated by measuring the respective electromagnetic fields. Based on triggered lightning data, the U.S based National Lightning Detection Network (NLDN) network uses an empirical formula for the estimation of lightning peak current. The empirical formula proposed by Rakov et al. [20] to estimate negative return-stroke peak current is inferred from 28 lightning triggered data and is given by (2.3):

I_{EF}=1.5-0.037rE Eq. 2.3

Where I_{EF} is the return stroke peak current in kA, E is the electric field peak in V/m, and r is the distance to the lightning channel in meter. Similarly, a new empirical formula (2.4) derived by Mallick *et al.* is based on 91 negative strokes from 24- rocket and wire-triggered lightning flashes.

I= -0.74-0.028rE Eq. 2.4

The one proposed by Uman and McLain in 1969 [21] to estimate the lightning peak current is based on a transmission line model, is represented by (2.5):

$$I_{Tl} = \frac{2\pi\varepsilon_0 c^2 r}{v} * E \quad \text{Eq. 2.5}$$

Where ε_0 is the permittivity of space, c is the speed of light and v is the return stroke velocity of the lightning (one-third to two-thirds of the speed of light [22]).

2.2.3 Lightning Current Waveform

In addition to the return stroke peak amplitude, several other characteristics must be considered: maximum current derivative, average current rate-of-rise, current rise time, current duration, total charge transfer, and action integrals (energy transfer). Figure 2.1 depicts the lightning current waveform and its constituent characteristics.

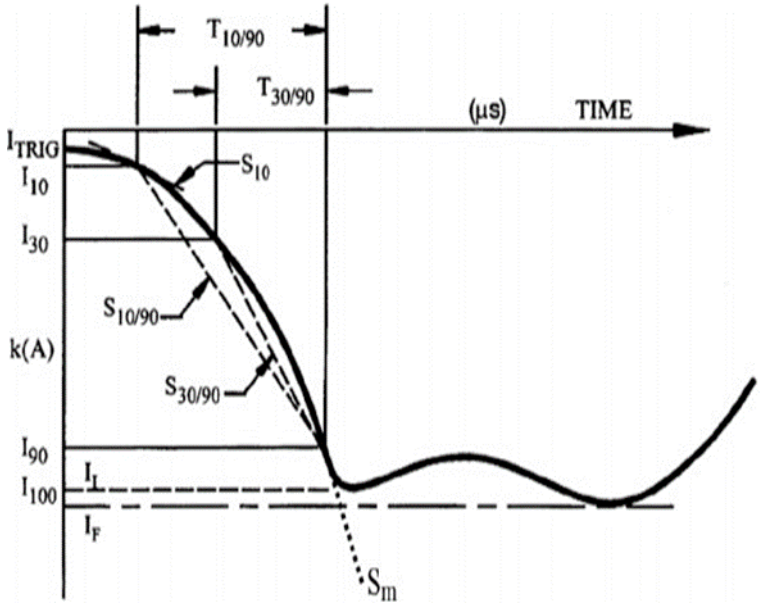

Figure 2.1: Lightning current waveform (adapted from [23])

2.3 Impacts of Lightning

Electrical power from high voltage substations is transmitted to end users through distribution networks. The voltage levels in distribution networks range from a few to 40 kV [24]. Distribution networks are classified into two groups based on their construction: overhead and underground. Underground distribution networks are specifically constructed in highly populated areas. Because they are buried beneath the earth's surface, such networks are particularly vulnerable to indirect lightning. Overhead lines, on the other hand, are vulnerable to both direct and indirect lightning strikes. Direct lightning strikes occurs on one of the distribution line's phase conductors. Indirect lightning is the phenomena that occurs when a lightning return stroke strikes near the distribution network, causing overvoltage stress on phase conductors. In this research our main concern is towards direct lightning strokes. Figure 2.2 depicts two types of lightning effects in distribution network: physical damage and insulation failure.

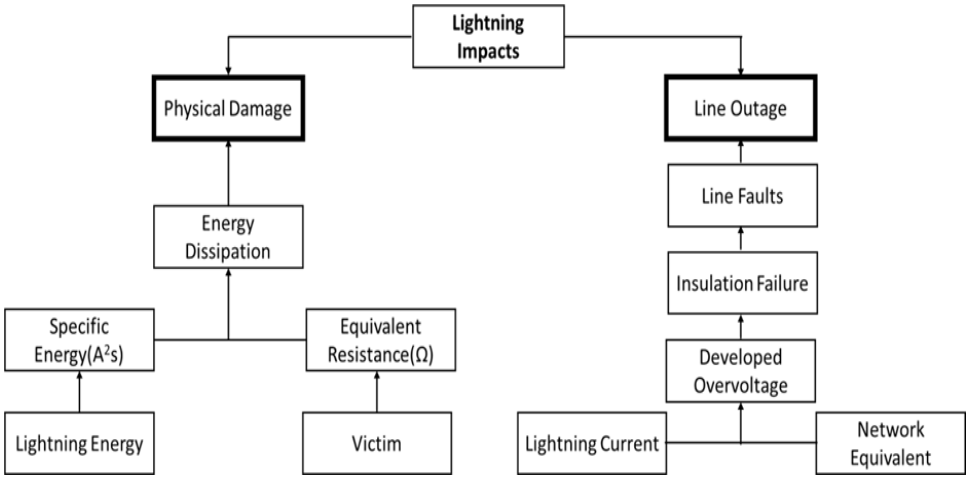

Figure 2.2: Impacts of lightning in overhead distribution networks

2.3.1 Physical Damage

It predicts the likelihood of damage occurring in any of the network components individually or in combination. This type of impact occurs when lightning energy dissipates in a network component, which is commonly referred to as the victim. The victims are basic distribution network components such as line insulators, conductors, poles, crossarms, substations, distribution transformers, and residential and industrial appliances. The degree of physical damage is determined by the victim's equivalent resistance and the specific energy of the lightning stroke(s), with dissipated energy being the product of those two quantities. The value of specific energy changes with the type of lightning stroke, but the victim's equivalent resistance varies with material composition. The majority of physical harm is inflicted by direct lightning strokes, with only a few caused by indirect ones. The physical damage caused by indirect lightning is frequently preceded by insulation failure, as observed in sensitive equipment in low voltage installations.

2.3.2 Insulation Failure

It is explained by the phenomenon known as disruptive discharge, in which insulation fails to function due to electromagnetic stress caused by produced overvoltage. Unlike physical damage, insulation failures can be caused by both direct and indirect lightning strikes. Direct lightning occurs when the leader stream strikes one of the phase conductors directly; when the phase conductor potential exceeds the ground potential, the line insulation separating these two potentials may fail to insulate, resulting in normal flashover. Sometimes shield wires, if exists, fail to intercept the lightning return

strokes and the lightning directly hits the phase conductor instead; the insulation failure in such a condition is specifically termed as shielding failure flashover. Unlike flashover, the other way around, a back flashover is the condition where the insulation failure is due to ground potential being greater than the phase conductor potential. Back flashover results from direct lightning intercepted by ground wires/shield wires.

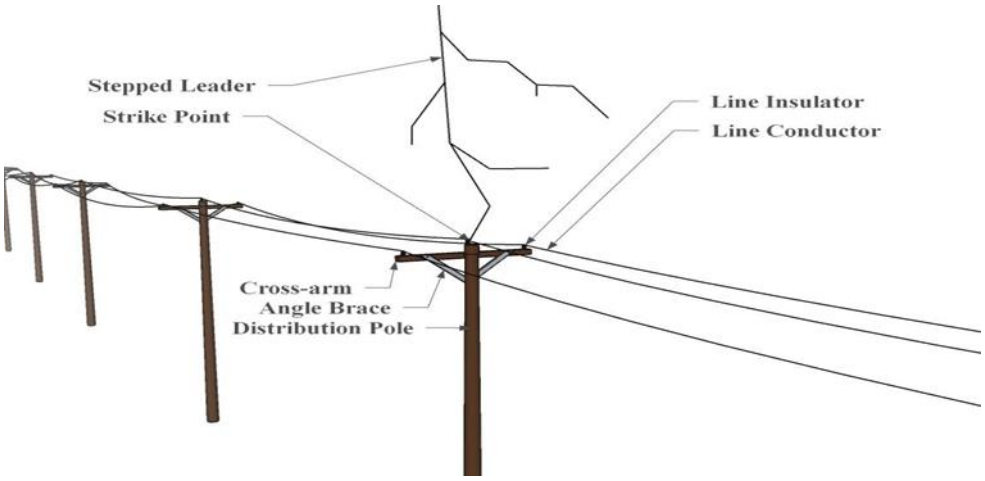

Figure 2.3: Direct lightning in overhead distribution line [25]

The degree of developed overvoltage depends on both the lightning-related parameter and the victim parameter (struck object). Based upon the insulation withstand capability of the victim object, the chances of insulation failure are defined accordingly. On the other hand, it is seen that the amplitude and the waveshape of the developed overvoltage which causes insulation failure, is directly related to the return stroke current parameters. During direct lightning events, the peak of developed overvoltage majorly depends on the peak magnitude and the time-to- peak value of the return stroke current. The wavefront (time to peak) of the lightning current also determines the nature of the lightning overvoltage wavetail. In addition to that, the ground impedance of the struck object and its distance from the strike point determine the time to half value of the overvoltage. In contrast to High Voltage (HV) lines, MV lines with low insulation levels are the victim of both first and subsequent strokes of direct lightning. Moreover, the insulation failure in MV lines is mostly due to nearby flashes, as direct lightning is more likely to be intercepted by taller objects. Even if the strikes are intercepted by nearby objects/open ground, electromagnetic stress is experienced by the MV network explained by Field-to-Line Coupling, which beyond the electrical strength would result in insulation failure. The induced voltage due to nearby flashes is mainly described by

the time-varying magnetic field of the lightning return stroke current. The lightning parameters which influence the induced overvoltages are the magnitude of lightning current peak current (I_{pk}), the time to peak (t_f), the waveshape (dI/dt), and the propagation velocity (b). In terms of insulation failure due to nearby flashes, first strokes with high peak current are as equally threatening as subsequent strokes with steeper current waveform [26], [27]. The other factors determining the overvoltage profile are soil resistivity, soil permittivity, height of the line conductors above the ground, and observation point and strike point location. The relation of these factors with the overvoltage has been listed in Table 2.1.

Table 2.1: Factors affecting overvoltages due to direct and indirect return strokes

<table>
<tr><th>Cause</th><th>S. N</th><th>Involved Parameter</th><th>Relationship with the Overvoltage [28], [29], [30]</th><th>Remarks</th></tr>
<tr><td rowspan="2">Direct Lightning</td><td>1</td><td>Return Stroke Peak Current (I_{pk})</td><td>The higher the return stroke peak current is, the higher will be the overvoltage peak.</td><td rowspan="5">1. The overvoltage peak for steeper return strokes is comparatively higher.
2. With finite soil conductivity, the magnitude of the second peak is greater than the first one.
3. The delay in overvoltage peak is seen, as the soil resistivity and the steepness of the return stroke current increases.
4. The induced overvoltage peak is comparatively higher for the soils with lower conductivity; however, the relation is opposite if the observation is made away from the stroke</td></tr>
<tr><td>2</td><td>Soil Resistivity (ρ) and Grounding Resistance (R_g)</td><td>The higher the soil resistivity and the grounding resistance are, the higher will be the overvoltage peak.</td></tr>
<tr><td rowspan="3">Indirect Lightning</td><td>1</td><td>Steepness of the Current Wavefront (t_f)</td><td>The higher the steepness of return strokes, the higher will be the overvoltage peak.</td></tr>
<tr><td rowspan="2">2</td><td rowspan="2">Return Stroke Propagation Velocity (b)</td><td>The higher the propagation velocity, the higher will be the overvoltage peak(t_f=1μs)</td></tr>
<tr><td>The higher the propagation velocity, the lower will be the overvoltage peak(t_f=3μs)</td></tr>
</table>

Cause	S. N	Involved Parameter	Relationship with the Overvoltage [28], [29], [30]	Remarks
	3	Conductor Height above the Ground (**h**)	The higher the conductor height above the ground is, the higher will be the overvoltage peak.	location. 5. For wavefronts with different steepness, an anomalous relationship between b and V_{pk} is seen. 6. If the lightning strikes close to a line termination, negative overvoltage peaks can also be seen near another line termination. 7. The difference in overvoltage peak for different soil permittivity is not much significant.
	4	Observation Point (**x**)	The farther the observation point is, the lower will be the overvoltage peak.	
	5	Soil Resistivity (**ρ**)	The higher the soil resistivity is, the higher will be the overvoltage peak**(x=1000m)**	
			The higher the soil resistivity, the lower will be the overvoltage peak.	
	6	Permittivity of Soil (ε_r)	The higher the soil permittivity, the lower	

2.4 Protection Against Lightning

When the produced overvoltage exceeds or equals the Critical Flash Over (CFO) of a line insulator, flashover is possible. As previously stated, overvoltage occurs as a result of a direct hit from a lightning return stroke or from adjacent flashes. Almost all direct strikes result in line flashovers, regardless of the protection strategy; however, line flashovers caused by indirect hits can be reduced by using a variety of protective schemes. The number of line flashovers per 100 km per year is commonly used to assess line performance. There are three methods for improving line performance: boosting line insulation withstand capability (CFO), utilizing regularly grounded shield-wires, and installing line arresters. As per the site requirement and cost function, these ways can be adopted separately or combined.

2.4.1 Increased CFO Protection

CFO is the statistically determined voltage level (insulation level) which when exceeded on an insulator indicates a 50% probability of flashover. The line flashover

rates in distribution lines can be decreased by increasing the CFO. The desired CFO level for the specific site must be considered before commissioning distribution networks. A preliminary study of the specific site can be carried out for the selection of an appropriate type of insulator, crossarm, and pole.

2.4.2 Shield-Wire Protection

Shield-Wire (SW) protection includes a shield wire at the top of towers above the phase conductors, as shown in Figure 2.4, which runs through the entire distribution network. The effectiveness of SW protection is very limited in the case of direct lightning, as there exists a chance of backflashover even if it intercepts a direct hit to the phase conductor. So, for the protection against direct hit backflashover, it is suggested to have low grounding resistance and sufficient CFO. However, the use of shield wires against indirect lightning can be proven beneficial as the magnitude of induced overvoltages gets reduced due to its application, with lower chances of flashovers [28]. The reduction in the number of induced flashovers is explained by the phenomenon known as 'capacitive coupling'. The greater the coupling is, the more is the reduction in induced overvoltage, and the less is the chance of flashover.

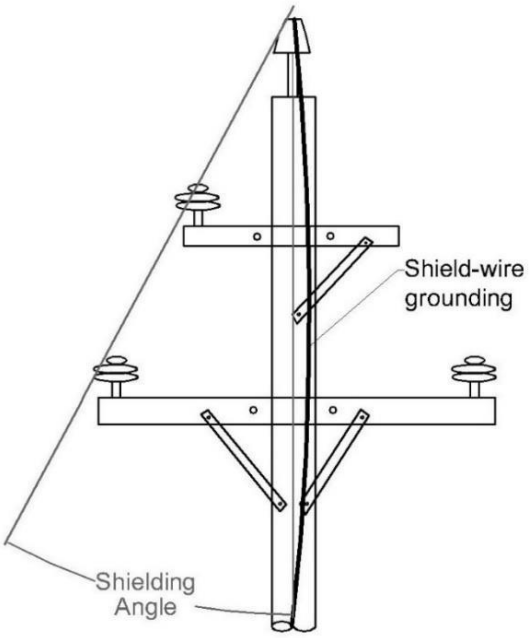

Figure 2.4: Shield-wire protection [25]

The effectiveness of shield wire protection in any distribution line is assessed by using a ratio termed as 'shielding factor', which is the ratio of induced voltage on the phase conductor in the case of SW protected lines to the case of unprotected ones. The relation

of different factors affecting the effectiveness of SW protection is tabulated in Table 2.2.

For perfect shield wire protection, one should be aware of the shielding angle provided by a particular arrangement. It is suggested to have a shielding angle less than or equal to 45^0 for towers smaller than 15m with conductor spacings less than 2m [31]. EGMs are used for the design of shield wire protections. As already been discussed, it is necessary to attain the required insulation of the overall structure, if needed, secondary insulation shall be added. Likewise, it is also mandatory to attain the grounding resistance as low as possible for the better effectiveness of the shield wire. Since more direct lightning is attracted towards hybrid configurations, and the separation of the distribution line phase voltage to the shield wire is comparatively high, the resulting coupling voltage is low. Specifically, for the distribution network underbuilt HV network, ground resistance and CFO level should be well taken care of.

Table 2.2: Factors affecting the effectiveness of SW protection

<table>
<tr><th>S.N</th><th>Factor</th><th>Remarks [28]</th></tr>
<tr><td>1</td><td>Distance between the Line and the Stroke Location (d)</td><td rowspan="6">The effectiveness of SW protection increases as:
1. the stroke location moves farther from the line. 2. the soil conductivity increases.
3. the ground resistance decreases. 4. the shield-wire height increases.
5. the strike point gets near to the grounding point. (best when in front)</td></tr>
<tr><td>2</td><td>Soil Resistivity (ρ)</td></tr>
<tr><td>3</td><td>Ground Resistance (R_g)</td></tr>
<tr><td>4</td><td>Height of the Shield Wire above the Ground (h)</td></tr>
<tr><td>5</td><td>Grounding Spacings (x_g)</td></tr>
<tr><td>6</td><td>Strike Point Location with respect to Groundings</td></tr>
<tr><td>8</td><td>Steepness (t_f)</td><td rowspan="2">The effectiveness of SW decreases with the increasing propagation velocity for high-resistivity soils and slower current wavefronts and increases another way round.</td></tr>
<tr><td>7</td><td>Propagation Velocity (b)</td></tr>
</table>

2.4.3 Arrester Protection

The application of surge arresters (SA) in distribution lines is another way to protect from lightning impacts. As sketched in Figure 2.3, distribution transformers and poles can be equipped with lightning surge arresters to improve performance. Lightning surge arresters protect the equipment insulation and prevent circuit interruption initiated by flashovers. Lightning surge arresters are nothing but a non-linear resistance kept between the phase conductor and the grounding lead. Lightning arresters conduct surge current to the ground; and also limit the voltage across the terminal it has been connected to, which is the sum of the discharge voltage of the arrester and the developed inductive voltage. The developed overvoltage on an unprotected pole for a lightning strike hitting the midspan between the same and a protected pole is determined by using the separation distance (l), the arrester- discharge voltage (VIR), the wave velocity (c), the line surge impedance (Z_0), and the rate of rising of voltage (a function of the front time, t_f), as in (2.6).

$$V = V_{IR} + \frac{l}{c} * \left(I * \frac{Z_0}{2} * t_f \right) \qquad \text{Eq. 2.6}$$

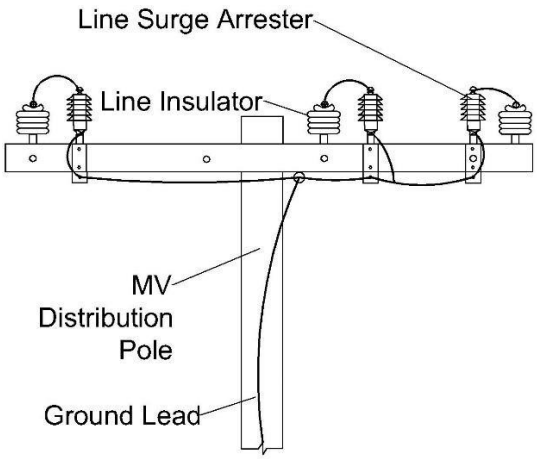

Figure 2.5: Arrester protection in distribution network [25]

Arrester protection for direct strikes becomes a challenging task with a high magnitude surge current, steep wavefront, and large energy content. So, arrester spacing plays a vital role in determining line performance. It is suggested to put arresters at all phases of every pole to achieve better lightning performance against direct hits. It has been noted that the flashover rate had increased from 70% to 80% by increasing the arrester spacing from two spans to three spans, for a distribution system with a span length of 75 m, CFO of 350kV, and grounding impedance of 10Ω [4]. Subsequently, for nearby

flashes, arrester protection is more prominently pronounced as the significant number of induced overvoltage line flashovers is reduced.

From a study of 83 km long 13.8 kV overhead distribution line with surge arresters in all phases on every 300m span, it was found that the number of lightning outages was reduced by 50% with the reduction of 75% of faults caused by indirect strokes [32]. Similarly, Paolone *et al.* [33] and Yokoyama *et al.* [34] found that a significant reduction in induced overvoltage can be achieved by using arresters on every phase in every 200m span; while Mc Dermot *et al.* suggested 360m span. Piantini and Janiszewski [35] suggested that it is not required to put an arrester on every phase, however, span length should be considered wisely. For better distribution line performance, Chen *et al.* have realized that the surge arrester spacing of 400m is required for low-insulation levels with high ground conductivity or high-insulation levels with low ground conductivity; while for low-insulation levels with low conductivity, it is required to reduce spacing to 200m [36]. In the year 2005, to account for cable laterals of MV lines as well, Hasmi *et al.* discussed the arrester installation scheme for the protection of MV cable laterals in terms of sub-lateral connections, and cable length. It has been found that due to cable attenuation a single arrester at the junction of overhead line and cable is sufficient for the protection of cable lengths more than 29 km or more [37].

The factors affecting the effectiveness of surge arrester protection have been listed in which need to be considered while devising distribution lines' lightning protection.

Table 2.3: Factors affecting the effectiveness of SA protection

S.N	**Factor**	**Remarks [28]**
1	Peak Current (**I_{pk}**)	1. Overvoltage decreases with the increasing current amplitude if $R_g < 50\ \Omega$, and the stroke location is in front of an arrester. 2. The effectiveness of the arrester protection increases as: i. Grounding resistance decreases ii. Arrester spacing decreases iii. Height of shielding nearby objects increases 3. Fluctuations in OVs are low for smaller arrester spacing and higher shielding object height.
2	Ground Resistance (**R_g**)	
3	Spacing between Arresters	
4	Height of Shielding Nearby Object	

Besides the factors discussed above for effective protection, it is essential to take notice of certain design parameters like discharge voltage characteristics, arrester rating, and arrester lead length. Before installing a particular line arrester, one should make note of discharge voltage characteristics as it determines discharge voltage for a particular stroke current which is to be seen at the equipment terminal. In addition to this, if the arrester lead length is unnecessarily long and discharge voltage is high, there exists a high chance of equipment failure and damage during the arrester operation. So, it is suggested to keep the arrester-distribution line separation and the ground-lead length to be as short and as straight as possible. Likewise, for better performance, it will be beneficial if arresters are installed specifically at poles with poor insulation: cutouts, dead-end poles, and crossover poles, also known as 'weak-links'. Sometimes, to have an economical MV line design, it is cheaper to have arresters on the top phase rather than on every phase. However, one should fulfill a higher insulation level in the unprotected one. A methodology named Direct Discharge Crossing (DDC) has been recently adopted to analyze the network criticality in terms of feeder lightning performance and realized the recommended location for lightning arresters installation [38]. Insulation coordination is another fact to consider while designing the arrester protection scheme. Insulation coordination is the study that makes sure which insulation flashovers first in an electrical network. To ensure proper lightning protection, the line designer must compare the Voltage-Current (VI) characteristic of the arrester and the parallelly connected component (insulator/transformer/generator). The component is assumed to be protected when the VI characteristic of the component is above the one that corresponds to that of the arrester.

2.4.4 Combined Protection

For places with high ground lightning activity, it is required to have a combined protection scheme with both shield wire and surge arresters, as depicted in Figure 2.6, in some cases, with the increased CFO as well.

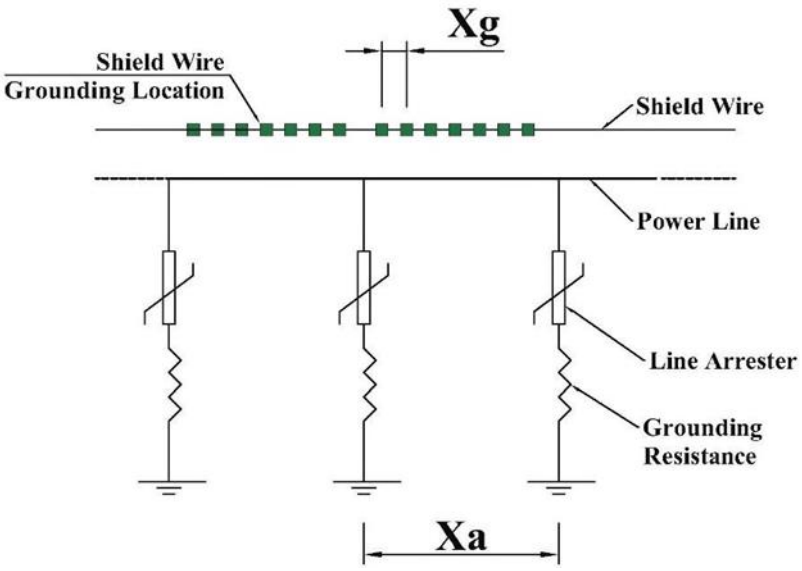

Figure 2.6: Combined shield-wire and surge arrester protection

Shield wire intercepts the lightning return stroke and diverts lightning current to the ground, while line arresters specially protect distribution lines from backflashover. If both are used with arresters on every pole and phase, it is expected that flashovers are virtually eliminated. Since lightning currents are diverted by shield wire, the combined protection scheme offers less energy duty to the arrester. With both SA and SW, the dependency on insulation level and grounding also get reduced.

For the protection of aerial cables from insulation puncture due to flashover from nearby shielding trees, enhanced insulation and adequately grounded shield-wire are required. In a risk-based insulation coordination study [39], for lightning-prone zones, it has been found that with combined protection of SA and SW, larger arrester spacing with alternate shield wire grounding can minimize the risk of insulation failure. The factors playing a major role in the lightning performance of distribution networks for different lightning protection measures are tabulated in table 2.5.

Table 2.4: Lightning performance with different types of protection

S. N	**Type of Protection**	**Factor**	**Remarks**
1	Unprotected Lines	CFO	Lightning Performance of distribution lines get can be improved: 1. with higher Critical Flashover Voltage (CFO) of line insulators
		ρ	
2	Shield Wire Protected lines	CFO	
		ρ	
		X_A	

S. N	Type of Protection	Factor	Remarks
3	Surge Arrester Protected	CFO	2. with smaller arresters spacing 3. with smaller spacing between grounding points of shield-wire 4. with high soil conductivity 5. with shielding objects like trees, buildings near the lines 6. with MV line built under the HV lines
		ρ	
		X_A	
4	Presence of Shielding Nearby Object	-	
5	Hybrid Configuration (HV+MV)	-	

Table 2.5: Related literatures in lightning protection of distribution networks

Title	Authors	Published Journal	Main Findings
Distribution Network Impact Assessment with Geometrically Identified Strike Points	Nasib Khadka, Aayush Bista, Diwakar Bista, and Brijesh Adhikary	IEEE	For lightning arrester spacing between 500 m to 1000 m, there were abnormalities with the increasing arrester spacing.
Methodology for analysis of electric distribution network criticality due to direct lightning discharges	Raphael Pablo de Souza Barradas, Gabriel Vianna Soares Rocha, João Rodrigo Silva Muniz, Ubiratan Holanda Bezerra, Marcus Vinícius Alves Nunes and Jucileno Silva	MDPI	Direct Discharge Crossing (DDC) method analyzes the network criticality based on two main factors, which are the overvoltage magnitudes and the number of flashovers provoked by lightning discharges and defines a feeder lightning performance function that is used to indicate the recommended location for

Title	Authors	Published Journal	Main Findings
			lightning arresters' installation.
Calculation of Lightning Flashover Rates of Overhead Distribution Lines Considering Direct and Indirect Strokes	Jiming Chen and Mingxiao Zhu	IEEE	The insulation level should be more than 300 kV to effectively reduce indirect flashovers. For a line with low-insulation level about 150 kV above high conductivity ground or with high-insulation level about 300 kV above low conductivity ground, the spacing between arresters is best less than 400 m. But for a line with low-insulation level above low conductivity ground, it is better to reduce the spacing to 200 m.
Protection against lightning overvoltages in resonant grounded power	F. Napolitanoa, A. Borghettia, C.A. Nuccia, M.L.B. Martinezb,G.P. Lopesb, G.J.G. Dos Santos	EPSR	The results (using Monte Carlo Simulations) provide the preliminary basis to select the mini-mum spacing and number (per phase) of surge arrester in order to achieve

Title	Authors	Published Journal	Main Findings
distribution networks			the requested lightning performance level. They also show the advantages of the presence of a grounded wire. The characteristic and number per phase of surge arresters need to be adequately selected in order to take advantage of the relevant protection zone, as nearby lightning can induce dangerous voltage at both sides of a protection device

CHAPTER THREE: RESEARCH METHODOLOGY

3.1 Methodology

This study is targeted on alayzing the effect of lightning in isolated solar mini grid. To obtain the objective of research, the mini network is modelled and simulation is performed for various operating conditions.

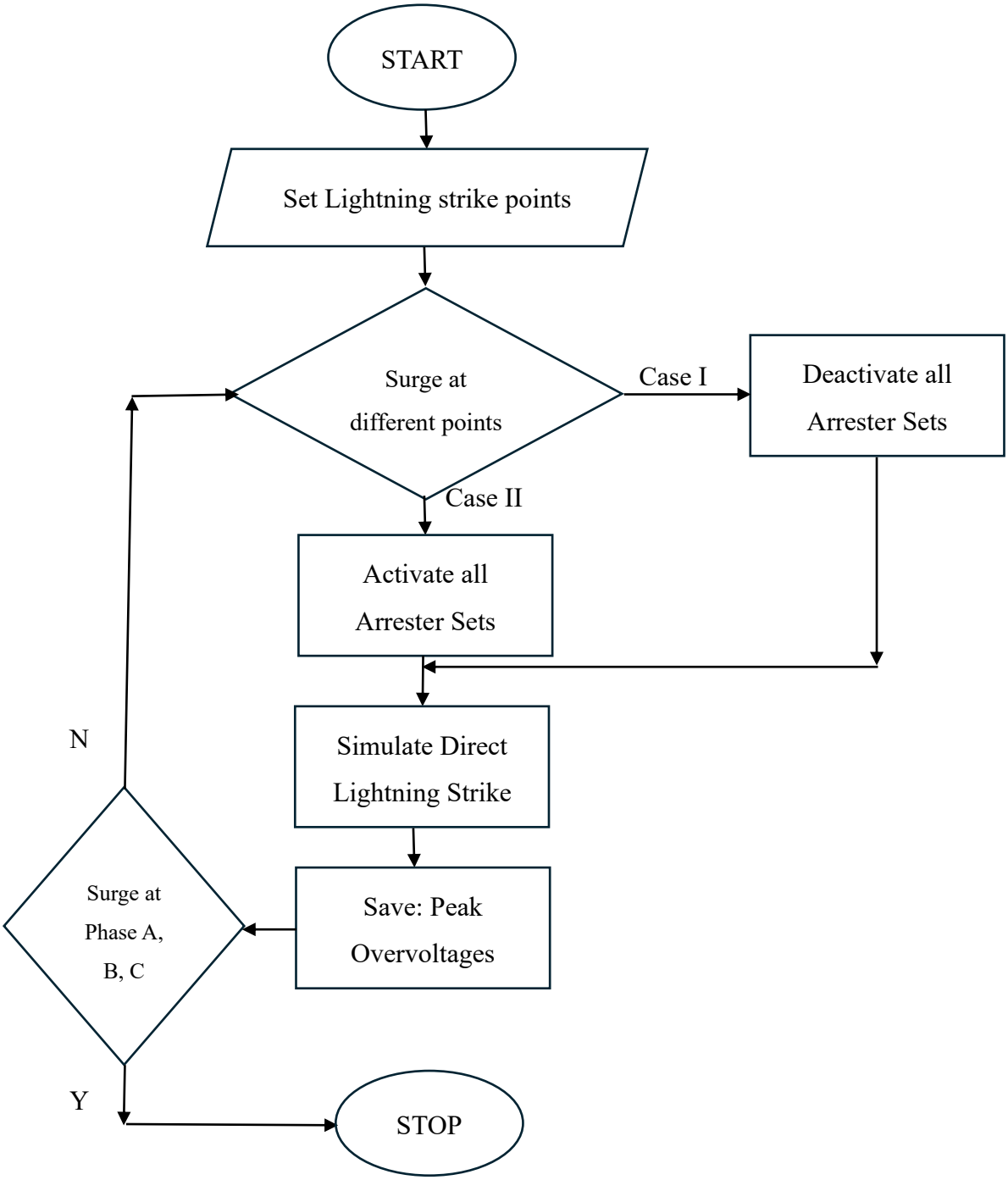

Figure 3.1: Methodology Flowchart

3.2 Modeling Techniques for Time-Domain Simulations

3.2.1 Solar Mini Grid Modeling

The solar PV system is simulated using the PV park model. The collector grid and PV inverters are represented using aggregated models. However, the model contains the park controller to maintain the PV park's overall control structure. The inverters and park control systems incorporate the essential nonlinearities, transient, and protection functions to accurately model the park's transient behavior in response to external power supply disturbances. The PV panel, the dc-ac converter system, the choke filter, the shunt ac harmonic filters, the PV array transformer and the PV park transformer are the components of the electrical systems EMTP diagram.

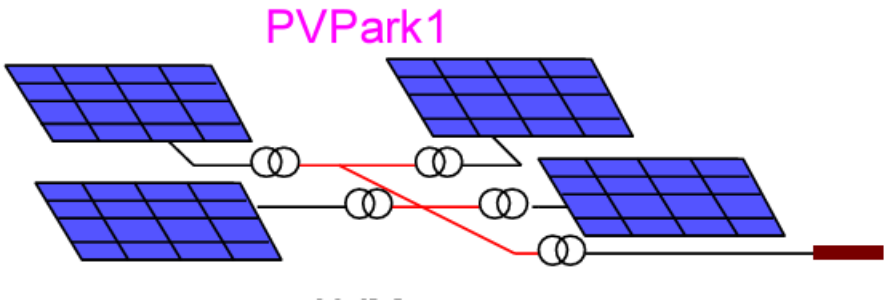

Figure 3.2: PV park used in EMTP simulation

3.2.2 Distribution Network Modeling

The line conductors of transmission and distribution networks for the electromagnetic transient study are modeled by using either Constant Parameter (CP), Frequency-Dependent (FD), or Universal Line Model (ULM). By considering the line parameters as constant, the CP model is the simplest and most efficient one in terms of computation. CP model shall be used for the lines farther from the lightning strike point. FD model accounts for the frequency dependence of the line conductors and can be used near the strike location. However, the accuracy of the FD model is limited to the cases of overhead lines with symmetric or nearly symmetric configurations. As the ULM model works directly in the modal domain, its application is extended to represent asymmetric overhead lines as well as underground cables. In this simulation FD model is used. This model is more accurate than the Constant Parameters (CP) line model. It is however computationally slower. Unlike the CP-line model the Frequency Dependent (FD) line

model takes into account the frequency dependence of R′ and L′ (series resistance and inductance of the line per unit length).

3.2.3 Modeling the Lightning Process

The standard lightning waveform adopted by IEEE 1159.1 2009 and IEEE C62-41.2 2002 standards [40] has a wavefront of rise-time 1.2μs and wavetail of 50% decay time at 50μs. A lightning source can be simply modeled with the combination of a step function and an exponential function to emulate the steep rise of the wavefront and the decaying wavetail [41], as in (3.1).

$$I(t)=Ae^{(-\alpha(|t-t1|))}.I(t-t_1) \quad \text{Eq. 3.1}$$

In the literature [42], it is discovered that the double exponential model has been used to describe the channel base equation in the majority of return stroke models. In contrast to the real concave rising section of the lightning current waveform, the double exponential function yields a convex rising portion. Heidler's model is better than the double exponential models since it takes into consideration the amount of charge transmitted, the rate of growth and the concave rising section. The current waveforms subsequent strokes are often realized by Heidler's function can be seen in the (3.2): [43], [44]

$$I(0,t)=\frac{I_0}{\eta}\frac{\left(\frac{t}{\tau_1}\right)^n}{\left(\frac{t}{\tau_1}\right)^n+1}e^{-\frac{t}{\tau_2}} \quad \text{Eq. 3.2}$$

The sum of two Heidler functions with different parameters can be used to represent the desired current waveform [45] more accurately. Even if the double exponential function gives an unrealistic convex waveform, it is sometimes used along with the Heidler function as in (3.3) for the calculation of lightning return stroke electric and magnetic fields [46]

$$I(0,t)=\frac{I_{01}}{\eta}\frac{\left(\frac{t}{\tau_1}\right)^n}{\left(\frac{t}{\tau_1}\right)^n+1}e^{-\frac{t}{\tau_2}}+I_{02}\left(e^{-\frac{t}{\tau_3}}-e^{-\frac{t}{\tau_4}}\right) \quad \text{Eq. 3.3}$$

CIGRE current source with the mathematical representation (3.4) as the wavefront and (3.5) as the wavetail can be used for simple and approximate results. A, B, t_1, t_2, I_1, and I_2 are constants derived from lightning parameters time to half, front time, maximum steepness, and current peak. Similarly, t_n is the instant of maximum steepness depending on exponent n; similarly,

$I_f = A + Bt^n$ Eq. 3.4

$I_t = I_1 e^{\frac{-t-t_n}{t_1}} - I_2 e^{\frac{-t-t_n}{t_2}}$ Eq. 3.5

3.2.4 Lightning Channel

Experimental results indicate that the equivalent channel impedance ranges between several hundred ohms to a few kiloohms. Similarly, the impedance perceived by lightning at the strike point ranges from many tens of ohms or less [18].

3.2.5 Equipment Modeling

3.2.5.1 Surge Arrester

SA is designed in such a way that it must be able to withstand power frequency voltage, temporary overvoltages, slow front overvoltages, and fast front overvoltages. The commonly used surge arresters are of two types: non-gapped (NGLA) and externally gapped (EGLA). For transient simulations, it is necessary to observe the energy duty of the SA under lightning stress, such that the system design is done to avoid the probable energy breakdown. According to IEEE WG 3.4.11, for lightning studies, it is suggested to use the high-frequency dependent model comprising RL component with RLC filter, as shown in Figure 3.3. The values of R0 (Ω), L0 (μH), C (pF), R1 (Ω), and L1 (μH) can be computed using (3.6), where d is the estimated height of the arrester (m) and n is the number of columns of metal-oxide in the arrester. It is to be noted that the value of L1 needs to be adjusted by changing its coefficient such that the modeled network should validate the arrester discharge voltages for 8/20 μs lightning current. While A0 and A1 behave as Zinc Oxide varistors whose resistance varies according to the respective VI curve of the SA.

$R1=65.\ d/n$; $L_1=15.\ d/n$; $L_0=0.2.d/n$; $R_0=100.\ d/n$; $C=100.\ n/d$ Eq. 3.6

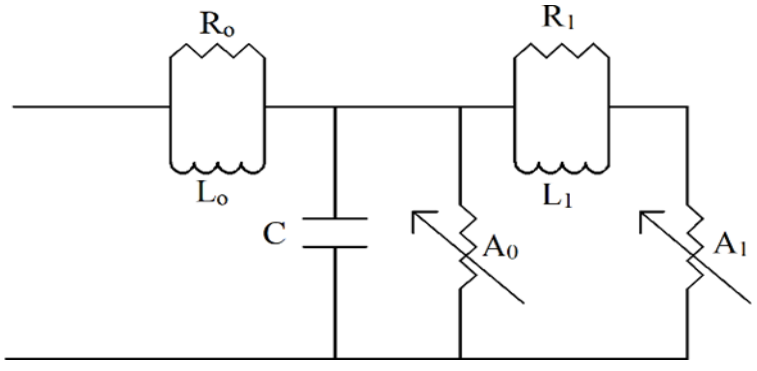

Figure 3.3: Line Surge Arrester (IEEE Model)

3.2.5.2 ZnO Data Function Device

The ZnO arrester data function device is used to generate the model data needed for the EMTP ZnO arrester model (ZnO device). The model data is generated from the actual current-voltage characteristic of the arrester available from manufacturer tests. This Model Data Calculation function uses the following form of the exponential describing the protective characteristic of a ZnO arrester:

$$i_{km} = p\left(\frac{v_{km}}{V_{ref}}\right)^{q} \qquad \text{Eq. 3.7}$$

where i_{km} (from k side to m side) is the arrester current, v_{km} is the arrester voltage and V_{ref} is an arbitrary reference voltage (arrester's MCOV, for example) used to prevent numerical overflow problems for large voltage values. The arrester current-voltage characteristic is fitted by one or more exponential functions, each valid in a particular range. The exponential segments are fitted on a log-log plane (straight line segments) to avoid numerical ill-conditioning of the exponential fitting. The resulting mathematical model of the arrester is shown in Figure 3.4. Each segment j is described by its own version of the above exponential function:

$$i_{km} = p_j\left(\frac{v_{km}}{V_{ref}}\right)^{q_j} \qquad \text{Eq. 3.8}$$

Below the first exponential start voltage V_{min1} the arrester is assumed to be linear. The arrester may have a gap which changes its characteristic upon sparkover. It is possible to enter separate data for the characteristic after sparkover.

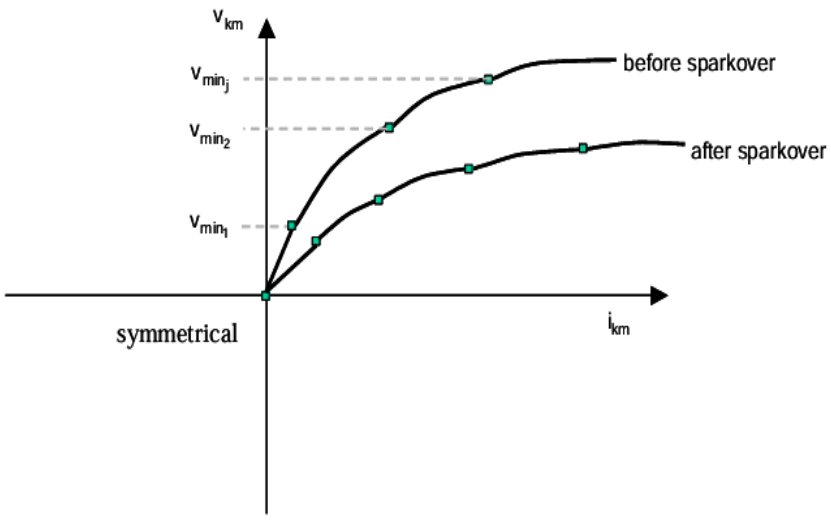

Figure 3.4: Zinc Oxide arrester characteristic

3.3 Electromagnetic Transient Program – Restructured Version (EMTP-RV)

A simulation program called EMTP is used to research transients in large-scale electrical networks and power systems. The method for putting together network equations used by EMTP is based on sparse modified-augmented-nodal analysis. Using a Jacobian-based nonlinear solver, topological constraints are removed enabling the solution of extremely large-scale nonlinear systems with the fewest possible iterations [47].

For this study, EMTP has been used to find the overvoltages and currents at different nodes/ branches, when lightning return stroke current is injected at any point of the designed medium- voltage network.

3.4 Conclusion

By using the models discussed in this section, time-domain simulations can be carried out for lightning protection studies of isolated solar mini grids.

CHAPTER FOUR: OVERVOLTAGE IMPACT ASSESSMENT IN A SOLAR MINI GRID

4.1 Introduction

Overvoltage's occur at distribution network nodes during both direct and indirect lightning strikes. The overvoltage during direct lightning is caused by the lightning return stroke acting as a current source in the victim network. The size of the overvoltage at the strike point is determined by the equivalent surge impedance detected and overvoltages at subsequent nodes are measured using the transferred surge current. This section covers how to measure the impact of overvoltage on the case study network. Time domain simulations are run on the user selected direct strike sites. The simulations are carried out using electromagnetic transient program.

4.2 Description of Case Study Solar Mini Grid

The mini-grid site is located within Sinja Rural Municipality, Ward No-5, Sanagau village, Jumla District of Karnali Province. The geographical coordinates of the proposed site are 29°18'51.58"N 82° 1'24.32"E located at an elevation of 2720 meters. The mini-grid service is demanded for the existing 183 households of nearby village toles, some public service energy demands within the service area. The daily load curve estimate of the village shows 18 kW peak demand during evening, where the maximum connected loads can go up to 35.75kW. The projection shows an estimated average daily energy demand will be 161.9 kWh in the base year 2023. The resource assessment conducted through one of the best available tool of Global Solar Atlas called 'Solargis' shows global horizontal irradiation (GHI) of Sanagau village is 5.5 kWh/m^2/day and with 33 degree optimum tilt angle towards south direction, the global tilted irradiation (GTI) is observed to be 6.38 kWh/m^2/day. The village has got adequate solar PV generation potential where average specific PV energy output will be 5.11 kWh/kW_p per day. 60 kWp solar PV system with 6.52 Km (without service cable) is used to meet estimated daily energy demand of the end users. using three phase and single-phase power supply.

Considering the provision mentioned in Electricity Regulation, 2050, dog conductor is used in distribution system to reduce voltage drop within permissible range. This regulation is crucial for maintaining the stability and reliability of the electrical power supply. It ensures the voltage level remains within acceptable range, preventing

potential damage to electrical equipment, reducing the risk of power outages and promoting the efficient operation of the electrical grid.

Table 4.1: Salient features of solar mini grid

Headings	Particulars	Description
User community	Name	Sanagau User Community
Category	Project Name	Sanagau Solar Mini Grid
	Capacity(kWp)	60.0
Location	GPS coordinate	29°18'51.58"N 82° 1'24.32"E
	Altitude	2740
	Province	Karnali
	District	Jumla
	Rural Municipality	Sinja RM-05
	Village	Sanugau
	Route	Kathmandu-Surkhet-Narkot-Sinja
	Distance of the nearest black topped road	90 km Manma
	Distance of the nearest gravel road	500mts
	porter distance	500 mts
	Nearest electrified site	7 Km from NEA grid
Consumers	Households	183
	Businesses	5 projected
	Anchors	4
System sizing	Solar insolation	6.384 kWh/m2/day
	Type of PV module	Si-poly/mono with an minimum efficiency of 18%
	Each module capacity	500 W
	Efficiency of module	18%
	Total number of modules	120
	PV array capacity	60.0
	Inverter type	PV
	Inverter capacity	50.0
	Inverter type	Battery inverter
	Capacity of inverter	27.0
	Type of battery	Lead acid sealed battery
	Individual battery capacity	2000AH 2V
	Number of batteries	96
	Battery capacity total	384.0

	230V single phase	4400
	Weasel(30 sq mm), km	0.00
	Dog conductor (100 sq. mm.), km	2.60
	Pole type and number	16.41
	410 SP-13 (8 meter)	58
	Daily energy generation kwh	119

Nepal's geographical feature combined with its location near the Bay of Bengal contribute to a higher likelihood of thunderstorms. Lightning is also more lethal in high mountains because it travels shorter distances to strike the ground. During the pre-monsoon season in Nepal, which lasts from March to June, convection systems caused by hot air rising from the Indian plains cause a lot of thunderstorms activity. Over 16 ground flashes occur annually in the southern area of Nepal, as seen in figure 4.1, which shows a significant ground flash density over the country. Department of Hydrology and Meterology of the government of Nepal has installed lightning detection sensors at different nine places: Tribhuvan International Airport, Tumlingtar Airport, Biratnagar Airport, Simara Airport, Bhairahawa Airport, Pokhara Regional International Airport, Nepalgunj Airport, Surkhet Airport and Attariya, Kailali district in 2018. This networks collects lightning data, location and time, which are very useful for the analysis of past events and future prediction. This network can detect the direction of thunderstorms for an hour and is thus valuable for lightning forecasting.

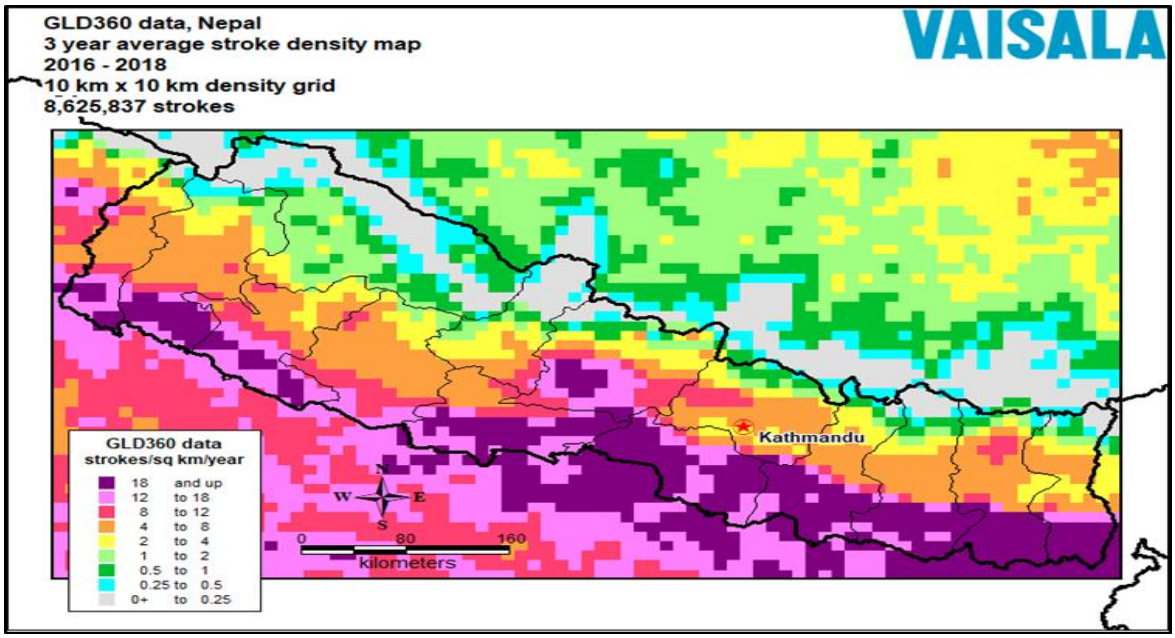

Figure 4.1: Ground flash density of Nepal (Source: VAISALA)

Figure 4.2 displays the single line diagram for the chosen case study.

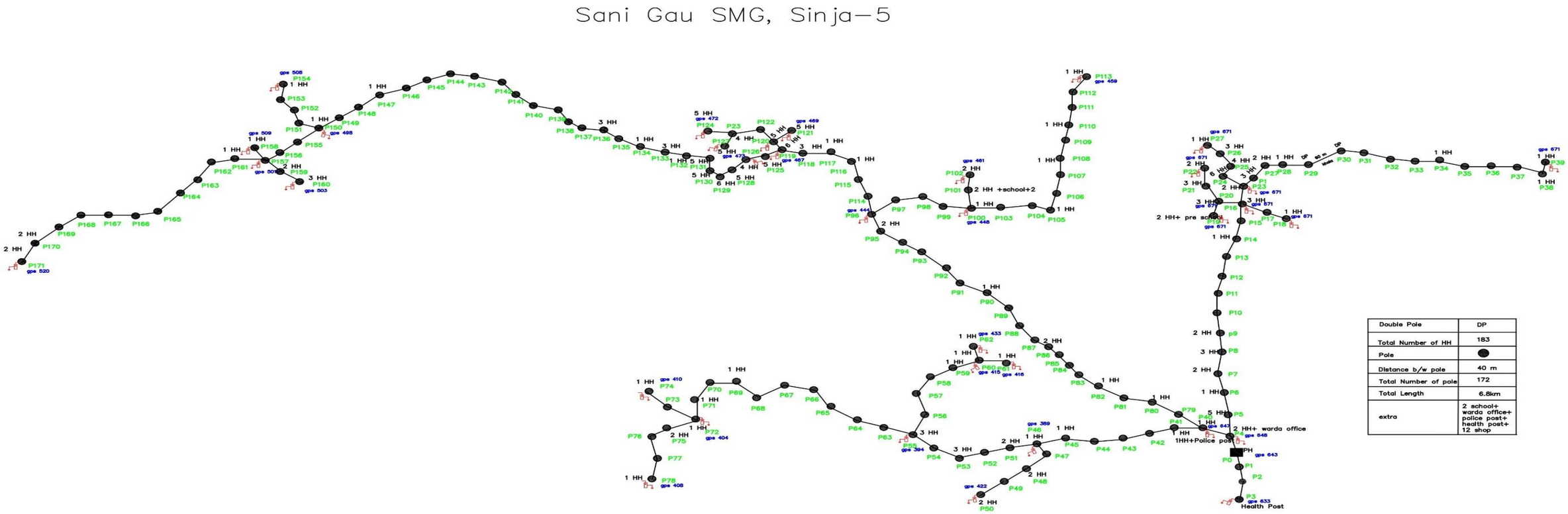

Figure 4.2: Single Line Diagram

The major system components that are chosen in the proposed solar mini grid power generation system are solar PV Modules, PV Inverter with inbuilt MPPT Controllers, Battery Inverters and Solar Deep Cycle Batteries. The proposed system has considered standard ratings of individual components to set up complete power generation units. Some of the standard components proposed in the system to be integrated in addition to items indicated above are PV mounting structures, cables and accessories, system protection units, lightning and earthing protection, monitoring and control units. The overall power generation system architecture is proposed in the following chapter of the single line diagram (SLD) of the power generation system.

The daily power and energy demand analysis and PV system design shows 161.3 kWh net amount of DC energy requirement of the village. It is estimated that a total of 120 numbers of 500 Wp (total 60 kWp solar PV array) can well serve the electricity demand of the village. The energy storage systems of 384 kWh can backup for 1.5 days autonomy, where a charge controller of 50 kW is recommended and the Battery Inverters of 27 kVA total capacity.

4.3 System Architecture

An DC coupled design topology is proposed for the 60 kW_p Sanagau Solar Mini Grid Project of Jumla district. PV and energy storage systems share an inverter with three or more interfaces when they are configured in a dc-coupled fashion. The converter has three interfaces: two on the dc side are for the PV and battery inputs, while a third on the ac side accepts an input from the utility grid. Power flows bidirectionally on the battery and utility interfaces but only unidirectionally from the PV array. Because DC coupling only requires a single power converter, it can be less expensive in terms of materials than AC coupling. In general, DC-coupled systems take significantly less physical area. DC coupling reduces energy loss since power is converted from DC to AC only once, compared to AC coupling. This type of architecture is suitable for small-scale community-based power systems. DC coupling technology in solar mini-grid systems offers a streamlined, efficient approach to integrating solar power and battery storage. It is well-suited for various applications, particularly in off-grid or remote locations where it can provide reliable and scalable power solutions. The single line diagram of the DC coupled solar PV mini grid system is presented in the below block diagram.

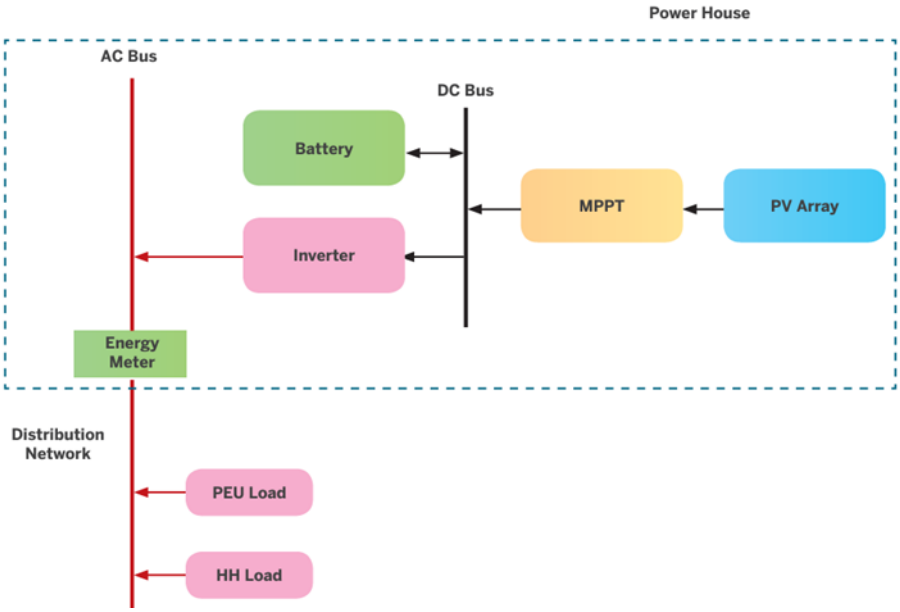

Figure 4.3: DC coupling topology of solar mini-grid power generation system

4.4 Direct Lightning Impact Assessment

Direct lightning events have been simulated for a set of strike points. The developed overvoltages at different clusters/locations are observed and subsequently analyzed.

4.4.1 Adopted Models, Input Parameters and Assumptions

For this case study, the T&D network was divided into 5 different clusters each consisting of 11-12 distribution poles as shown in figure 12. EMTP-RV software was used for carrying out simulations. Following are the specification of parameters adopted for this simulation:

Lightning Return Stroke Current

CIGRE lightning current source is used in this simulation study. The following are the values of the parameters utilized in this case study:

Table 4.2: Parameters of lightning current source

Parameters	Values
Start Time (t_{start})	0 s
Front Time (t_f)	1.2 µs
Maximum Current (I_{max})	100 kA
Maximum Steepness (S_m)	150 kA/µs
Time to half (t_h)	50 µs

Line Conductor

The frequency-dependent model proposed by J. Marti is used for this study. The spacing between the line conductors is shown in the table below.

Table 4.3: Values for line conductor

Phase	Resistance (dog conductor) (Ω/km)	Outside diameter (cm)	Horizontal distance(m) [a]	Vertical height (m) [b]
B	0.2733	1.415	-0.57	8.45
A	0.2733	1.415	0	9
C	0.2733	1.415	0.57	8.45

a. Negative refers to the left-hand side from the pole's center
b. Distance from ground level

Surge Arrester Model (High Frequency)

Table 4.4 shows the electrical and physical properties of surge arresters used in distribution lines. The non-linear resistance values are obtained from the manufacturer's datasheet VI characteristics and shown in table 4.5. The linear RLC branch values were computed using the method presented in (3.6) as per physical dimension and were found to be R_0 (18 Ω), L_0 (0.036 μH), R_1 (11.7 Ω), tuned L_1 (4.5 μH) and C (555 pf).

Table 4.4: 0.5 KV, 25 kA Surge arrester parameter

Parameters	Values	Parameters	Values
Nominal System Voltage	0.5 kV	Arrester Height (d)	180mm
Rated Voltage	0.38 kV		
Continuous Operating Voltage	0.42 kV	No. of Metal Oxide Columns in the Arrester	1

Table 4.5: Values of IV for non-linear resistance

For ZnO varistor A0		For ZnO varistor A1	
Current (I)	Voltage (V)	Current (I)	Voltage (V)
10	0.875	100	0.769
100	0.963	1000	0.850
1000	1.050	2000	0.894

For ZnO varistor A0		For ZnO varistor A1	
2000	1.088	4000	0.925
4000	1.125	6000	0.938
6000	1.138	8000	0.956
8000	1.169	1000	0.969
10000	1.188	12000	0.975
12000	1.206	14000	0.988
14000	1.231	16000	0.994
16000	1.250	18000	1.000
18000	1.281	20000	1.006
20000	1.313		

4.5 Time Domain Simulation

Two cases were considered for this assessment. The first case is the one where the modeled network is assumed to be unprotected: without any surge arresters. 100 kA CIGRE current source as a direct lightning impulse was injected on Phase A, Phase B and Phase C of cluster 5 only. A total of 36 observations were made and tabulated below. The case of overvoltage is at dead end low voltage clusters i.e. at cluster C1 and C8. Similar observations were also obtained for surge at other clusters.

Table 4.6: Observed overvoltage at different clusters without surge arrester

Lightning Surge Applied At (Without SA)	Surge Analysed At	Voltage Measured At (Phase)	Voltage (V)
Surge at Phase A of cluster C5	Cluster C9	va	4,696
		vb	553
		vc	518
	Cluster C1	va	38,086
		vb	2,937
		vc	1,536
		va	37,824

Lightning Surge Applied At (Without SA)	Surge Analysed At	Voltage Measured At (Phase)	Voltage (V)
	Cluster C3	vb	3,830
		vc	2,698
	Cluster C8	va	37,078
		vb	3,405
		vc	2,721
Surge at Phase B of cluster C5	Cluster C9	va	129,865
		vb	491,031
		vc	101,478
	Cluster C1	va	10,055,088
		vb	1,005,004
		vc	2,379
	Cluster C3	va	6,684,156
		vb	582,590
		vc	36,005
	Cluster C8	va	8,273,931
		vb	32,747
		vc	258,991
Surge at Phase C of cluster C5	Cluster C9	va	136,572
		vb	68,816
		vc	498,661
	Cluster C1	va	9,210,513
		vb	306,392
		vc	8,780
	Cluster C3	va	5,978,980
		vb	190,785

Lightning Surge Applied At (Without SA)	Surge Analysed At	Voltage Measured At (Phase)	Voltage (V)
		vc	25,492
	Cluster C8	va	7,143,947
		vb	15,733
		vc	100,595

The second case is the one with the surge arresters. 100 kA CIGRE current source as a direct lightning impulse was injected on Phase A, Phase B and Phase C at fifteen different locations. These locations were selected based on: the low voltage side (2clusters), the midsection of solar mini grid (2clusters) and near the power house. For each strike, peak overvoltage's were observed on all 3 phases.

Figure 4.4 shows the cluster division for applying lightning surges.:

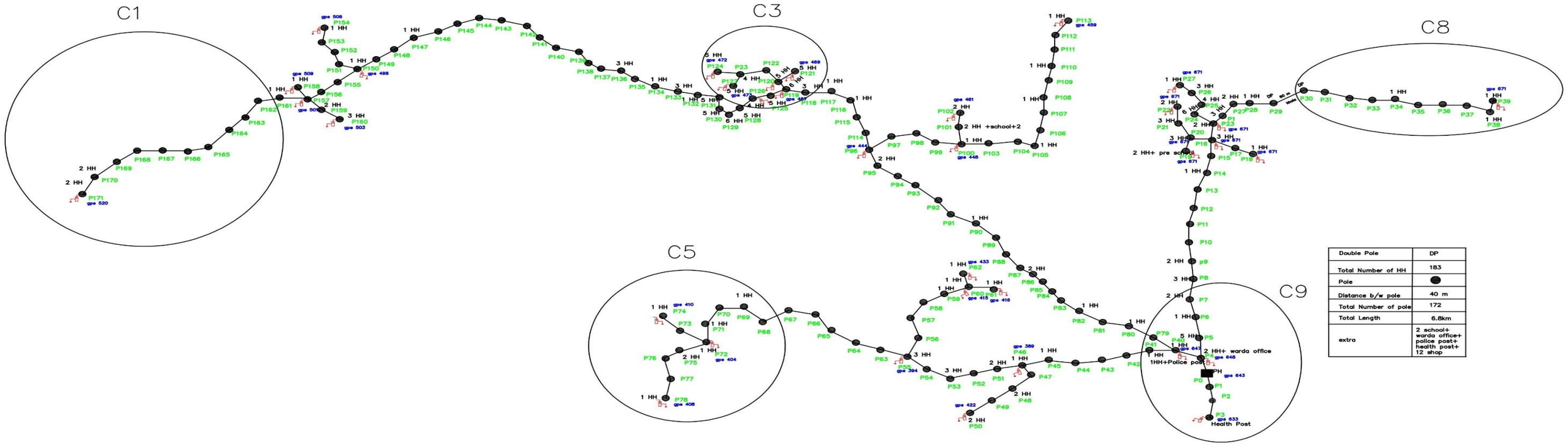

Figure 4.4: Distribution network cluster division.

Lightning overvoltage's were found at fifteen different stroke locations, with the majority occurring in low voltage clusters. Each direct strike resulted in 180 observations. The observations are tabulated below:

Table 4.7: Observed overvoltage at different clusters with surge arrester

Surge Applied At	Surge Analyzed At	Voltage Measured At (Phase)	Voltage (V)
Surge at Phase A of cluster C1	Cluster C9	va	14,279
		vb	6,272
		vc	6,615
	Cluster C3	va	864,140
		vb	110,101
		vc	16,859
	Cluster C5	va	10,901
		vb	216,356
		vc	199,613
	Cluster C8	va	891,681
		vb	37,731
		vc	48,955
Surge at Phase B of cluster C1	Cluster C9	va	2,089
		vb	11,004
		vc	2,348
	Cluster C3	va	99,813
		vb	407,151
		vc	25,550
	Cluster C5	va	2,519
		vb	105,300
		vc	33,948
	Cluster C8	va	82,001
		vb	147,951
		vc	59,963
Surge at Phase C of cluster C1	Cluster C9	va	505
		vb	399
		vc	1,147
	Cluster C3	va	18,114
		vb	9,635

Surge Applied At	Surge Analyzed At	Voltage Measured At (Phase)	Voltage (V)
		vc	44,375
	Cluster C5	va	1,647
		vb	2,999
		vc	10,056
	Cluster C8	va	16,496
		vb	8,335
		vc	39,859
Surge at Phase A of cluster C3	Cluster C9	va	31,775
		vb	6,721
		vc	9,959
	Cluster C1	va	1,201,650
		vb	433,494
		vc	20,334
	Cluster C5	va	25,699
		vb	261,247
		vc	226,596
	Cluster C8	va	1,289,297
		vb	86,678
		vc	429,758
Surge at Phase B of cluster C3	Cluster C9	va	2,956
		vb	35,274
		vc	5,699
	Cluster C1	va	326,395
		vb	1,192,543
		vc	10,040
	Cluster C5	va	4,412
		vb	594,907
		vc	134,370
	Cluster C8	va	201,758
		vb	255,716
		vc	333,116
Surge at Phase C of cluster C3	Cluster C9	va	990
		vb	636
		vc	12,255

Surge Applied At	Surge Analyzed At	Voltage Measured At (Phase)	Voltage (V)
	Cluster C1	va	43,894
		vb	106,602
		vc	46,512
	Cluster C5	va	2,869
		vb	51,736
		vc	87,188
	Cluster C8	va	195,212
		vb	20,192
		vc	696,084
Surge at Phase A of cluster C5	Cluster C9	va	3,957
		vb	527
		vc	502
	Cluster C1	va	33,937
		vb	2,706
		vc	1,347
	Cluster C3	va	32,355
		vb	3,316
		vc	2,353
	Cluster C8	va	32,381
		vb	2,903
		vc	2,388
Surge at Phase B of cluster C5	Cluster C9	va	5,435
		vb	18,316
		vc	2,250
	Cluster C1	va	190,410
		vb	72,390
		vc	1,450
	Cluster C3	va	92,220
		vb	24,666
		vc	3,613
	Cluster C8	va	117,333
		vb	23,925
		vc	28,672
	Cluster C9	va	5,389

Surge Applied At	Surge Analyzed At	Voltage Measured At (Phase)	Voltage (V)
Surge at Phase C of cluster C5		vb	1,141
		vc	16,209
	Cluster C1	va	190,221
		vb	12,048
		vc	5,187
	Cluster C3	va	89,233
		vb	6,317
		vc	13,976
	Cluster C8	va	108,916
		vb	2,833
		vc	32,460
Surge at Phase A of cluster C8	Cluster C9	va	19,143
		vb	7,346
		vc	6,139
	Cluster C1	va	1,074,824
		vb	442,138
		vc	10,757
	Cluster C3	va	957,706
		vb	107,719
		vc	39,907
	Cluster C5	va	19,540
		vb	388,241
		vc	338,207
Surge at Phase B of cluster C8	Cluster C9	va	548
		vb	5,006
		vc	525
	Cluster C1	va	60,686
		vb	227,375
		vc	8,222
	Cluster C3	va	64,112
		vb	207,340
		vc	18,220
	Cluster C5	va	3,592
		vb	51,605

Surge Applied At	Surge Analyzed At	Voltage Measured At (Phase)	Voltage (V)
		vc	10,124
Surge at Phase C of cluster C8	Cluster C9	va	2,122
		vb	1,797
		vc	11,267
	Cluster C1	va	54,848
		vb	165,924
		vc	34,317
	Cluster C3	va	62,754
		vb	92,600
		vc	166,431
	Cluster C5	va	2,442
		vb	47,322
		vc	19,260
Surge at Phase A of cluster C9	Cluster C8	va	796,170
		vb	7,101
		vc	20,328
	Cluster C1	va	1,025,073
		vb	98,912
		vc	1,789
	Cluster C3	va	680,907
		vb	27,064
		vc	6,059
	Cluster C5	va	26,208
		vb	321,597
		vc	277,749
Surge at Phase B of cluster C9	Cluster C8	va	583,276
		vb	32,687
		vc	116,441
	Cluster C1	va	803,541
		vb	393,311
		vc	1,619
	Cluster C3	va	435,789
		vb	127,686
		vc	5,598

Surge Applied At	Surge Analyzed At	Voltage Measured At (Phase)	Voltage (V)
	Cluster C5	va	9,485
		vb	1,127,447
		vc	356,751
Surge at Phase C of cluster C9	Cluster C8	va	540,183
		vb	4,634
		vc	339,759
	Cluster C1	va	929,350
		vb	156,612
		vc	6,492
	Cluster C3	va	474,513
		vb	55,177
		vc	30,041
	Cluster C5	va	9,209
		vb	387,383
		vc	1,132,838

An example of lightning overvoltage transients seen in other four clusters (C5, C3, C9 and C8) when surge is applied at phase A of cluster C1 is shown in figure below. For any potential stroke location, the cluster closest to the stroke location and dead-end low voltage sides always experiences the maximum overvoltage. The superposition of incident and reflected lightning current waveforms can explain this anomaly [39].

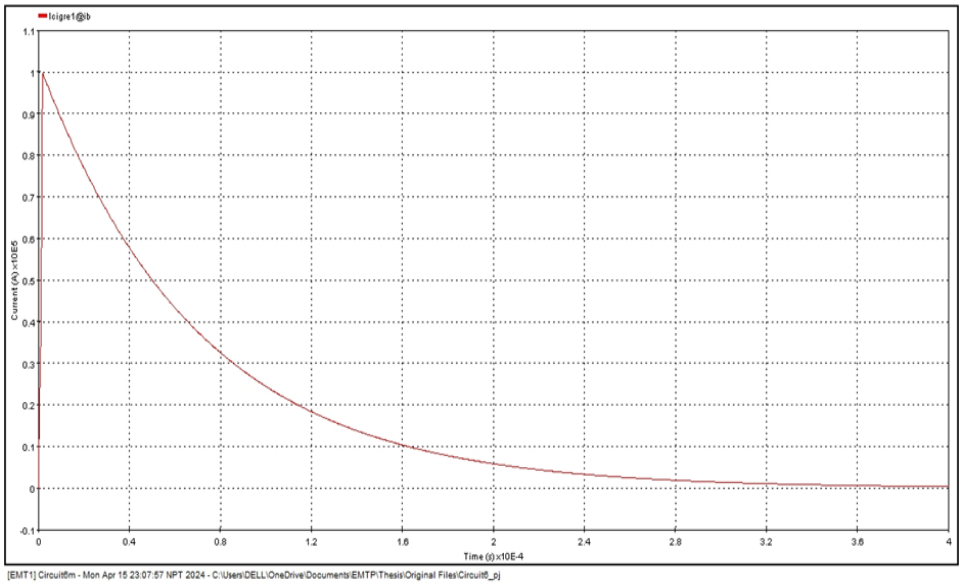

(a) 100 kA Lightning Current

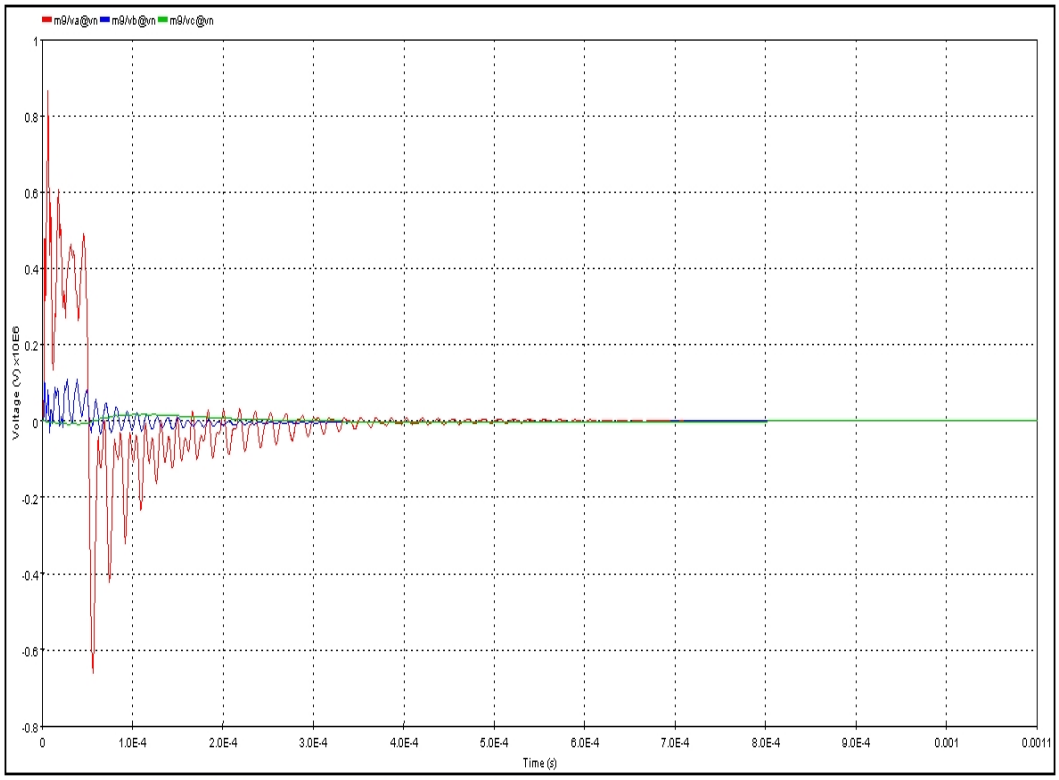

(b) Overvoltage at Cluster C3

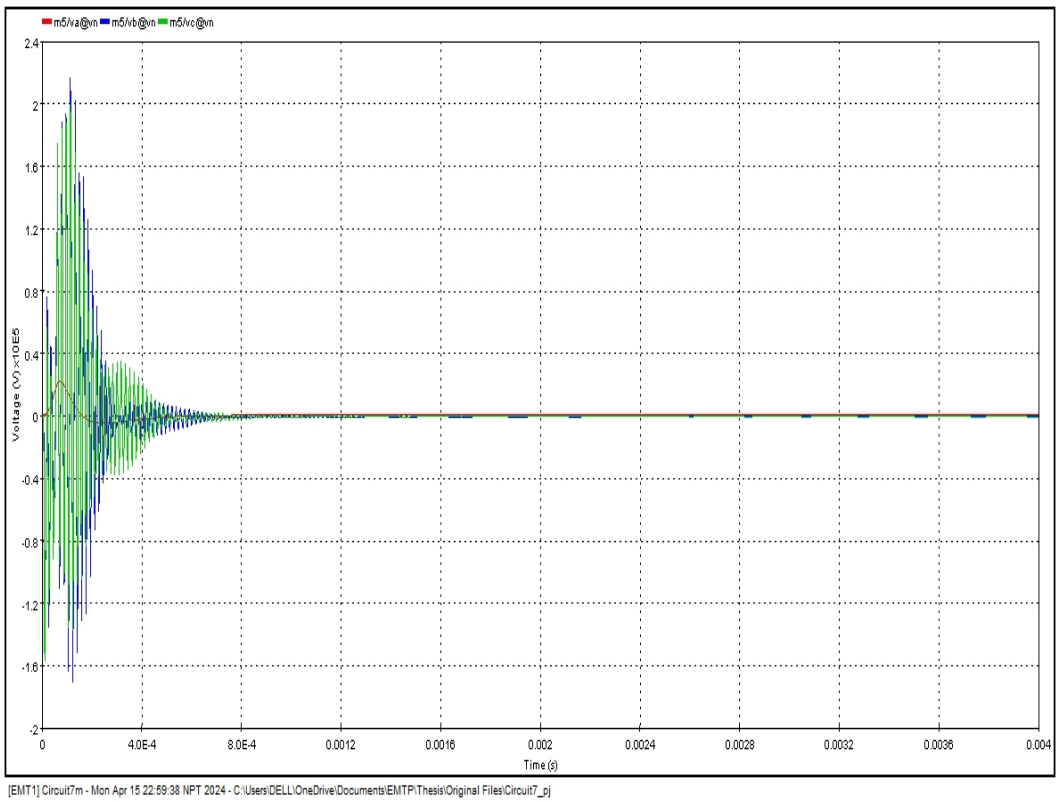

(c) Overvoltage at Cluster

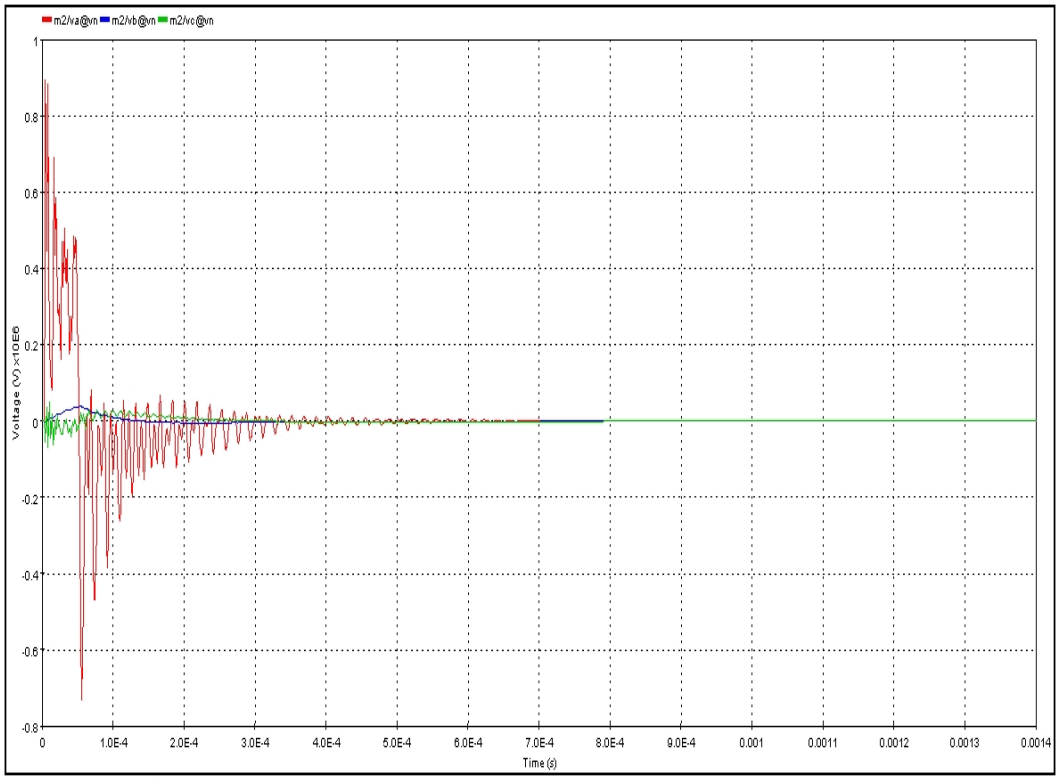

(d) Overvoltage at Cluster C8

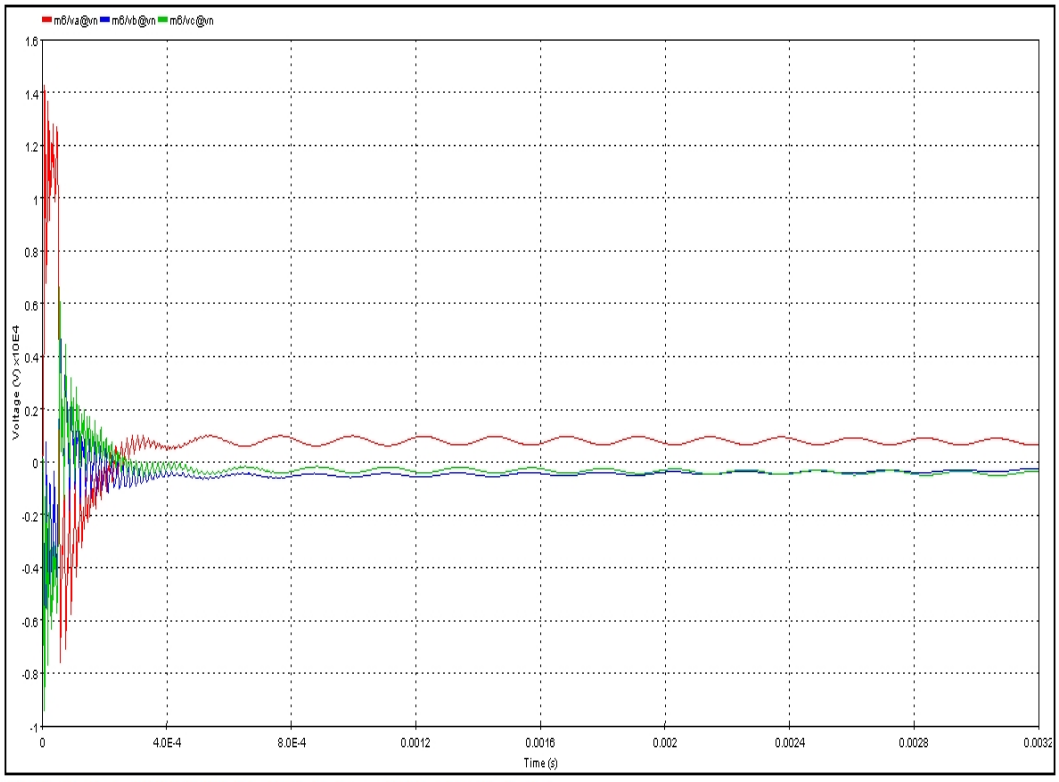

(e) Overvoltage at Cluster C9

Figure 4.5: Overvoltage at different clusters

4.6 Discussion and Findings

In this section, the critical clusters during direct lightning cases are analyzed.

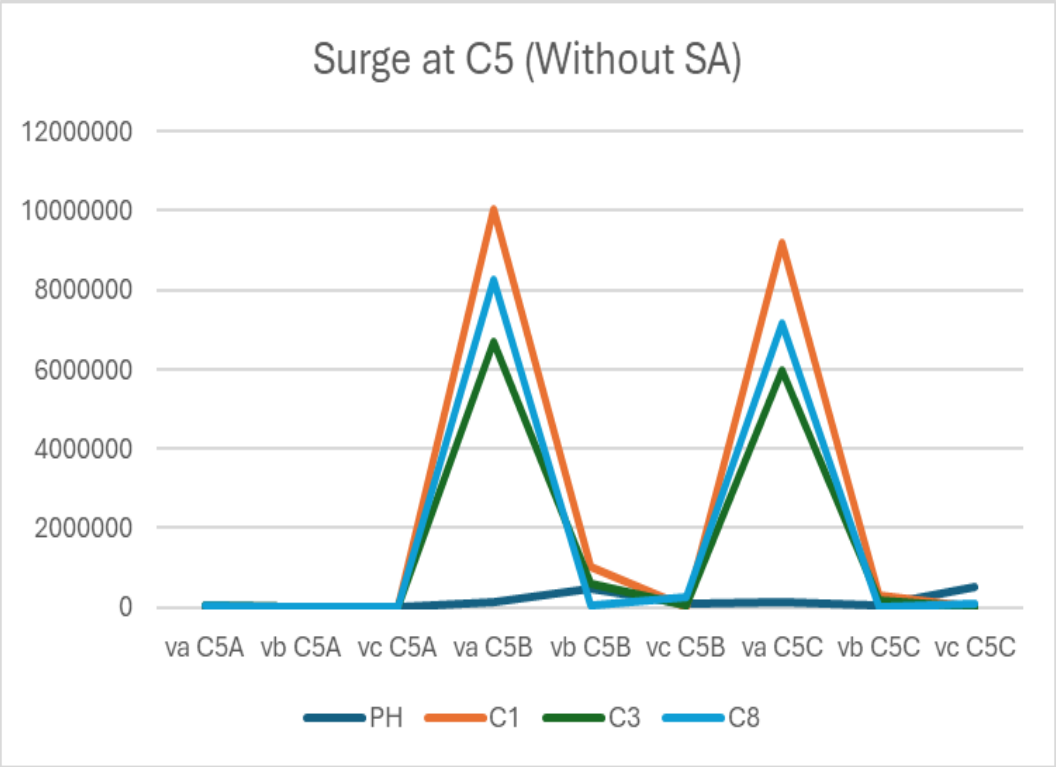

Figure 4.6: Overvoltage seen during lightning surge applied at cluster C5 without SA

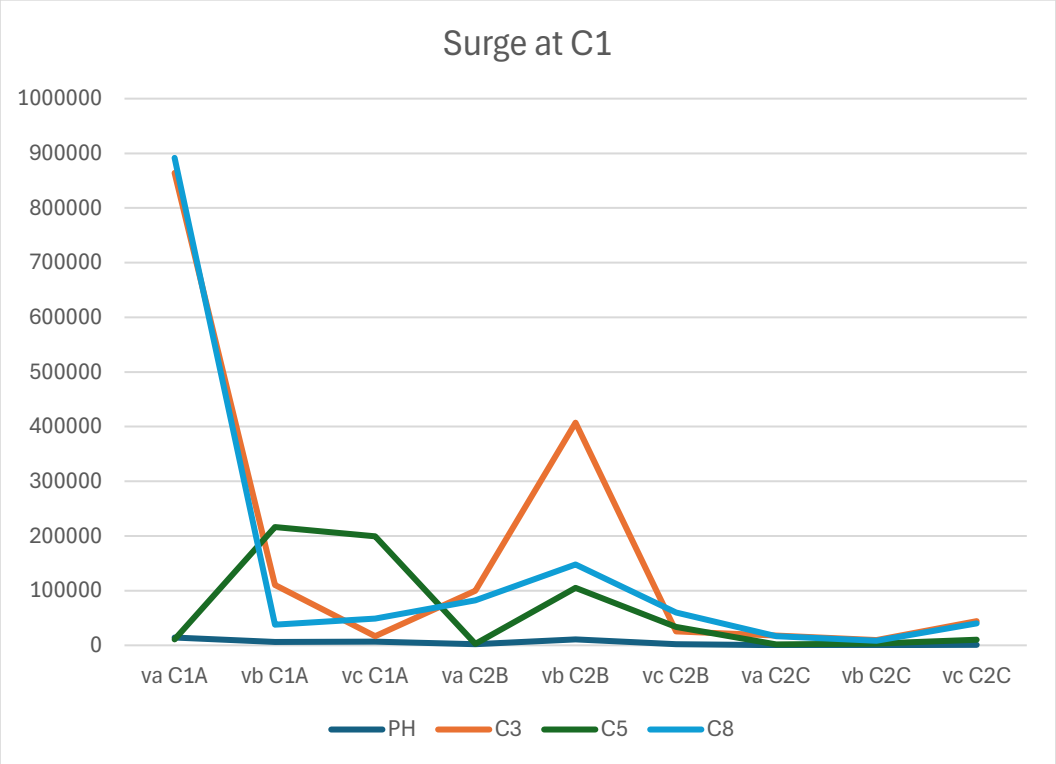

Figure 4.7: Overvoltage seen during lightning surge applied at cluster C1 with SA

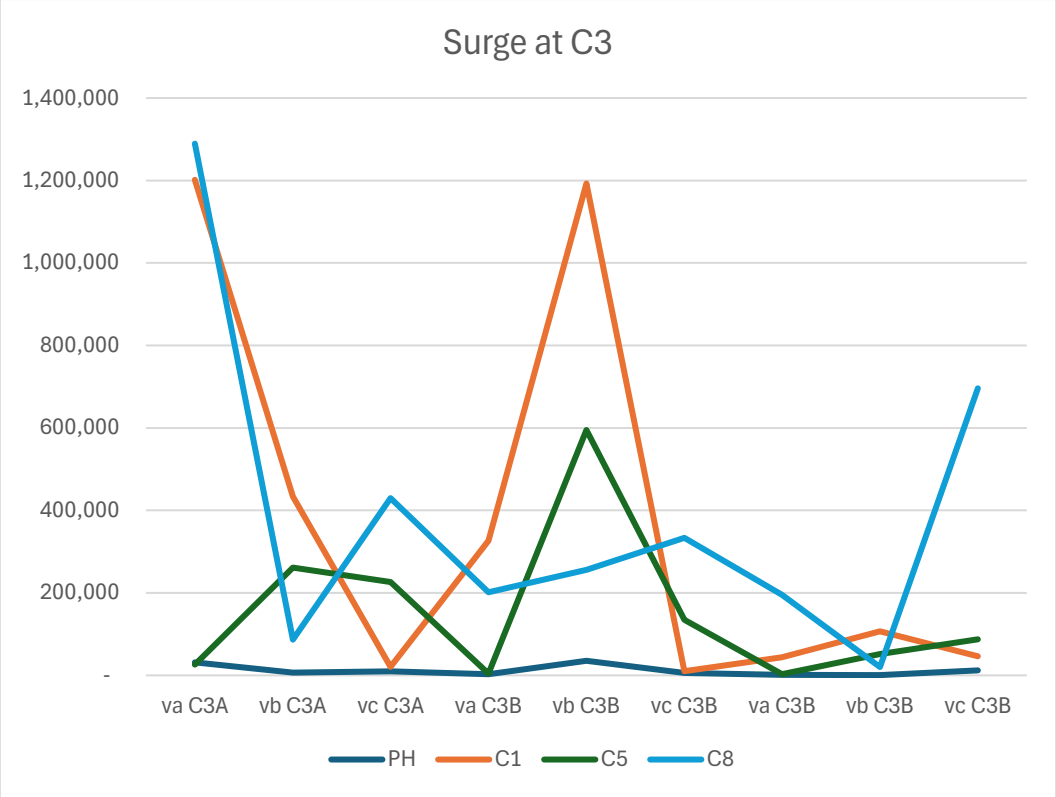

Figure 4.8: Overvoltage seen during lightning surge applied at cluster C3 with SA

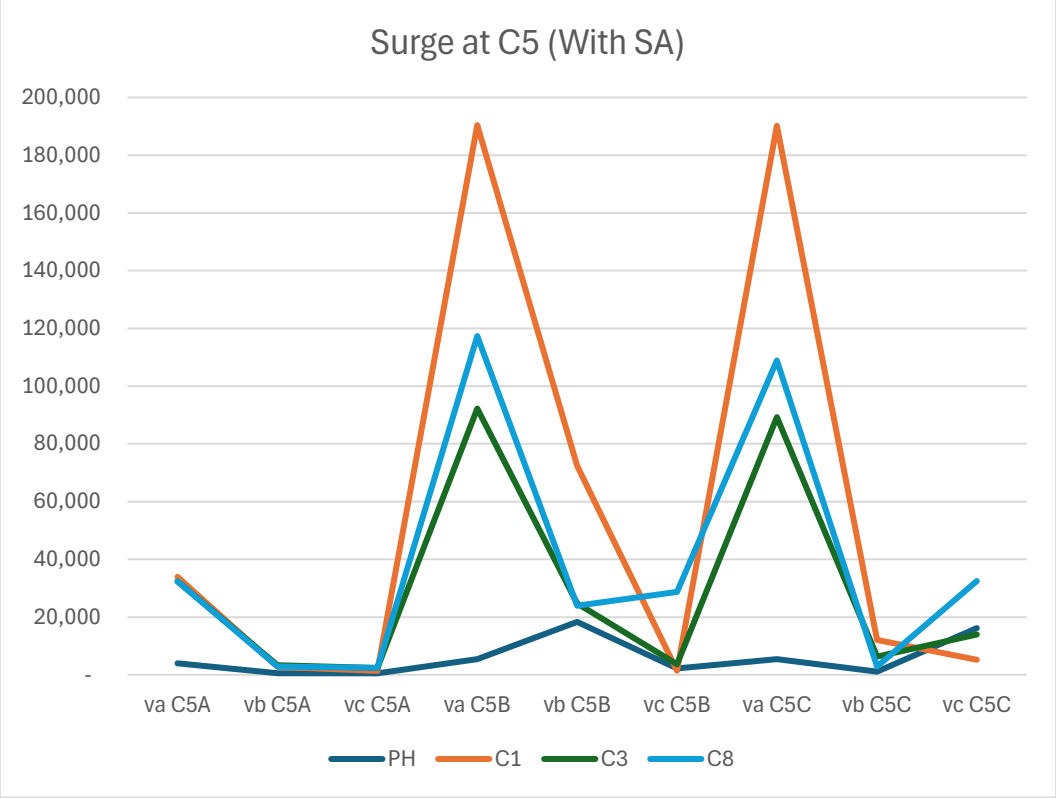

Figure 4.9: Overvoltage seen during lightning surge applied at cluster C5 with SA

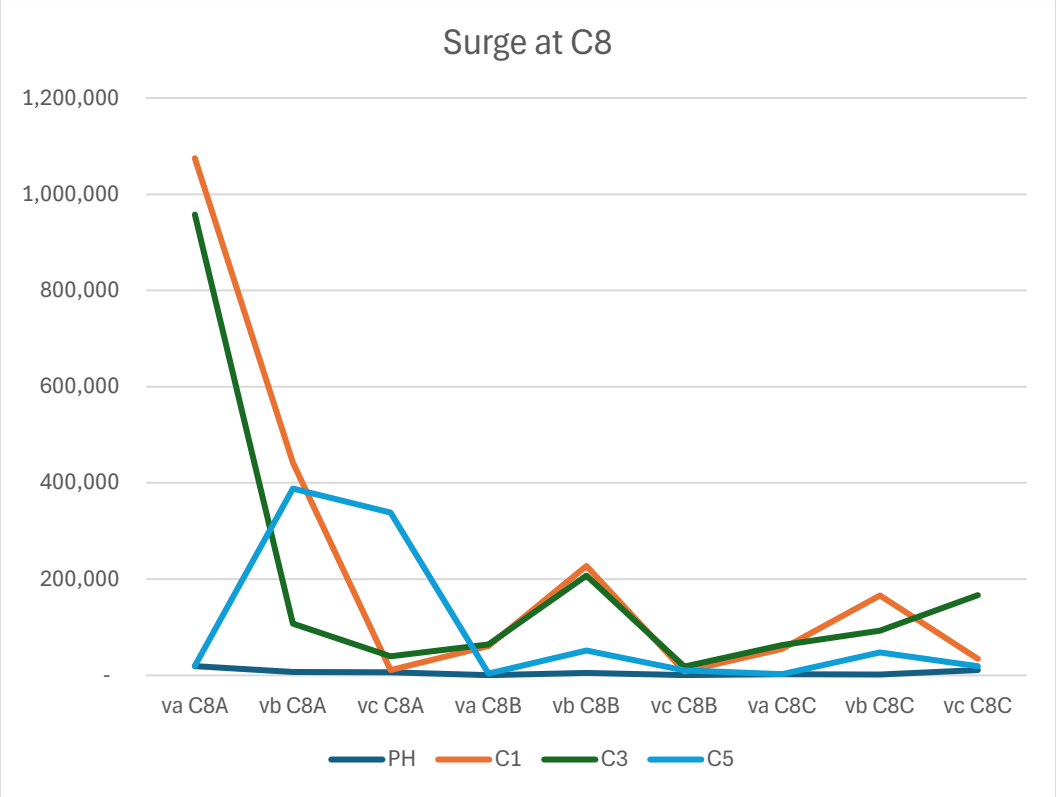

Figure 4.10: Overvoltage seen during lightning surge applied at cluster C8 with SA

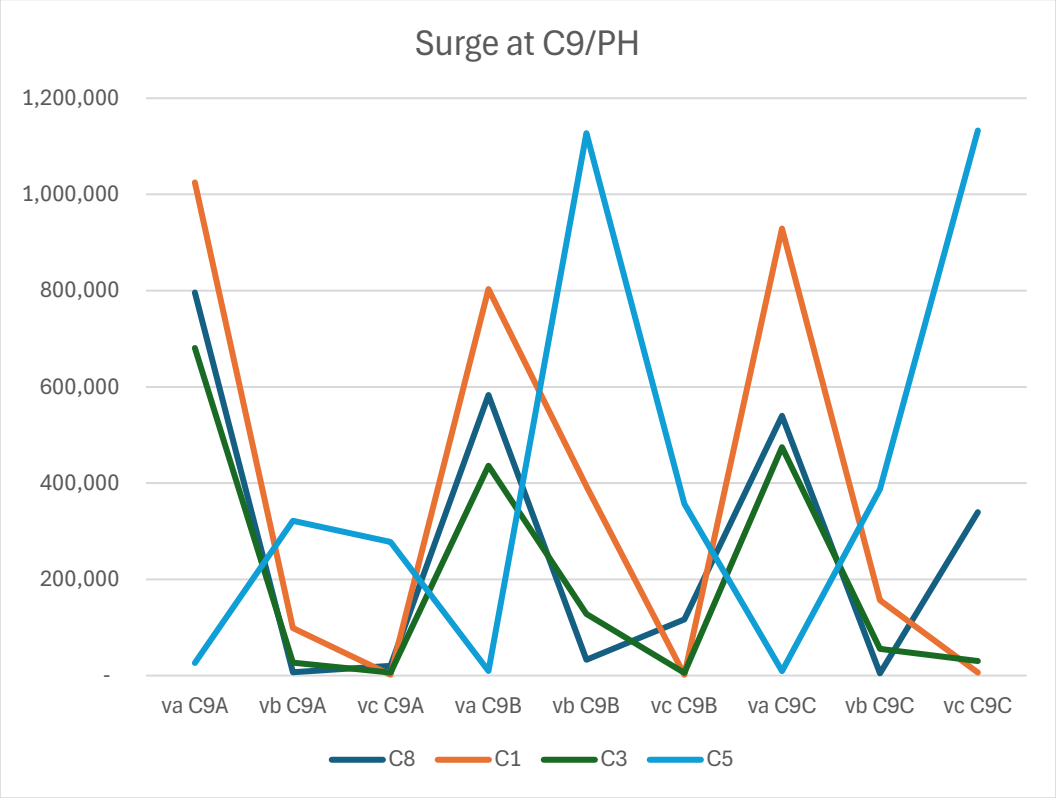

Figure 4.11: Overvoltage seen during lightning surge applied at cluster C9 with SA

For both protected (with SA) and unprotected (without SA) distribution network, critical clusters were those residing at the dead-end low voltage. The dead end low voltage clusters namely C1 and C8 were found to be most critical. In addition to the impedance observed at the specific node, traveling wave theory evidence can be used to explain the criticality of the dead-end LV side. The superposition of incident and reflected voltage waves may be the cause of the increased overvoltage growth at a particular node [39]. The impedance at certain nodes, particularly in dead end low voltage clusters, has a substantial impact on the level of overvoltage stress. Higher in impedance can result in higher voltage buildup, making these nodes more susceptible to lightning induced transients. At dead end clusters such as C1 and C8, the travelling wave strikes the line's end resulting in a powerful reflection. The reflected wave returns down the line and may interact with future incident waves. The combination of these incident and reflected waves might cause overvoltage at these nodes. The constructive interference of waves increases the voltage magnitude, making these clusters more vulnerable to overvoltage stress. In protected networks, surge arresters are installed to mitigate overvoltage by clamping the voltage to safe levels. However, surge arresters must be deliberate particularly near crucial clusters such as C1 and C8 to ensure effective protection.

CHAPTER FIVE: CONCLUSIONS AND RECOMMENDATIONS

5.1 Conclusions

By using EMTP software, a comprehensive representation of the entire solar mini-grid system including its distribution network is modeled. These models effectively describe the behavior and properties of solar panels, inverters, batteries and the distribution network. Using this program and model, transient analysis and system response under various situations, including lightning-induced transients, are performed. This model is critical for assessing the system's performance, analyzing its behavior under various scenarios, and developing efficient security methods.

The CIGRE current source model from EMTP is used to simulate lightning surges in the distribution system. Two cases, with and without surge arrester were analyzed. 15 different locations (for system with surge arrester) are chosen to introduce simulated lightning current waveforms into the system and observe their effects. This study aids in identifying potential system vulnerabilities and evaluating the efficacy of existing security solutions.

With appropriate modeling techniques for different components, the case study was simulated. In the case of system without surge arrester, 100 kA CIGRE current source as a direct lightning impulse was applied on Phase A, Phase B and Phase C of cluster 5. Maximum overvoltage of 10,055,088 V at cluster C1 and 8,273,931 V at cluster C8 were obtained. For the system with surge arresters, 180 observations were made from 15 different direct strike events across 5 different clusters. Table 4.5 shows that when the surge is applied and analyzed at Phase A of different clusters, critical locations were identified. For surge at cluster C1, the maximum overvoltage of 891,681 V was observed at cluster C8. Similarly for cluster C3, the maximum overvoltage observed at cluster C1 with 1,201,650 V and at cluster C8 with 1,289,297 V. Additionally, for surge at cluster C5, the maximum overvoltage at cluster C1 with 33,937 V and cluster C8 with 32,381 V. For surge at cluster C8, an overvoltage 1,074,824 V was observed at cluster C1. With surge at cluster C9 an overvoltage of 1,025,073 V and 796,170 V was observed at clusters C1 and C8 respectively. It has been discovered that during direct lightning events, the dead-end LV sides, cluster C1 and C8 are most impacted in terms of overvoltage stress. It can be concluded that additional arrester sets at the LV side of the distribution networks are needed for dead-end clusters.

The outcomes of this study imply that overvoltage stress is detected at specific locations during lighting studies, particularly for distribution networks.

5.2 Recommendations

During lightning strikes, the induced voltages and currents in the distribution networks are not uniform throughout the system. Specific places may incur increased overvoltage stress based on network topology, grounding resistance and the type of lightning strike. The simulation in EMTP software helps to identify these critical locations where the overvoltage stress is significantly higher. This could be due to the proximity to the lightning strike location, network setup or other local factors.

Uniform or regular placement of lightning arrester is not effective strategy in all cases. Based on the above simulation results, it is evident that a more strategic placement of lightning arresters can be achieved by analyzing the specific locations where overvoltage stress is highest. This ensures that arresters are deployed where they are most needed, offering targeted protection and lowering the arresters necessary.

Distribution network security can be considerably improved by using EMTP simulation findings to guide the strategic placement of lightning arresters. This strategy not only enhances network resilience but it also ensures optimal resource use, making it a cost-effective alternative for mitigating the effects of lightning induced overvoltages.

REFERENCES

[1] M. R. Patel, “Second Edition Design, Analysis, and Operation Wind and Solar Power Systems.”

[2] Conseil international des grands réseaux électriques. Comité d’études C4. and Impr. Conformes), *Lightning parameters for engineering applications*. CIGRÉ, 2013.

[3] K. N. Baral and D. Mackerras, “Positive cloud-to-ground lightning discharges in Kathmandu thunderstorms,” *Journal of Geophysical Research: Atmospheres*, vol. 98, no. D6, pp. 10331–10340, Jun. 1993, doi: 10.1029/92JD02844.

[4] D. Committee of the IEEE Power and E. Society, “IEEE Guide for Improving the Lightning Performance of Electric Power Overhead Distribution Lines Sponsored by the Transmission and Distribution Committee IEEE Power & Energy Society,” 2011.

[5] J. Kluss, M. R. Chalaki, W. Whittington, H. Rhee, S. Whittington, and A. Yadollahi, “Porcelain insulation – defining the underlying mechanism of failure,” *High Voltage*, vol. 4, no. 2, pp. 81–88, Jun. 2019, doi: 10.1049/hve.2019.0004.

[6] P. Heine, J. Turunen, M. Lehtonen, and A. Oikarinen, “Measured faults during lightning storms,” in *2005 IEEE Russia Power Tech*, IEEE, Jun. 2005, pp. 1–5. doi: 10.1109/PTC.2005.4524806.

[7] G. Medici, K. L. Cummins, D. J. Cecil, W. J. Koshak, and S. D. Rudlosky, “The intracloud lightning fraction in the contiguous United States,” *Mon Weather Rev*, vol. 145, no. 11, pp. 4481–4499, Nov. 2017, doi: 10.1175/MWR-D-16-0426.1.

[8] V. A. Rakov, *Fundamentals of Lightning*. Cambridge University Press, 2016. doi: 10.1017/CBO9781139680370.

[9] V. A. Rakov and M. A. Uman, *Lightning*. Cambridge University Press, 2003. doi: 10.1017/CBO9781107340886.

[10] N. Kitagawa, M. Brook, and E. J. Workman, “Continuing currents in cloud-to-ground lightning discharges,” *J Geophys Res*, vol. 67, no. 2, pp. 637–647, Feb. 1962, doi: 10.1029/JZ067i002p00637.

[11] V. A. Rakov and M. A. Uman, “Some properties of negative cloud-to-ground lightning flashes versus stroke order,” *Journal of Geophysical Research: Atmospheres*, vol. 95, no. D5, pp. 5447–5453, Apr. 1990, doi: 10.1029/JD095iD05p05447.

[12] “Some features of lightning flashes observed in Sweden,” *Journal of Geophysical Research: Atmospheres*, vol. 99, no. D5, pp. 10683–10688, May 1994, doi: 10.1029/93JD02366.

[13] “Characteristics of lightning flashes observed in Sri Lanka in the tropics,” *Journal of Geophysical Research: Atmospheres*, vol. 99, no. D10, pp. 21051–21056, Oct. 1994, doi: 10.1029/94JD01519.

[14] M. G. Ballarotti, C. Medeiros, M. M. F. Saba, W. Schulz, and O. Pinto, “Frequency distributions of some parameters of negative downward lightning flashes based on accurate-stroke-count studies,” *Journal of Geophysical Research: Atmospheres*, vol. 117, no. D6, Mar. 2012, doi: 10.1029/2011JD017135.

[15] A. C. V. Saraiva, M. M. F. Saba, O. Pinto, K. L. Cummins, E. P. Krider, and L. Z. S. Campos, “A comparative study of negative cloud-to-ground lightning characteristics in São Paulo (Brazil) and Arizona (United States) based on high-speed video observations,” *Journal of Geophysical Research: Atmospheres*, vol. 115, no. D11, Jun. 2010, doi: 10.1029/2009JD012604.

[16] Z. A. Baharudin, N. A. Ahmad, J. S. Mäkelä, M. Fernando, and V. Cooray, “Negative cloud-to-ground lightning flashes in Malaysia,” *J Atmos Sol Terr Phys*, vol. 108, pp. 61–67, Feb. 2014, doi: 10.1016/j.jastp.2013.12.001.

[17] R. Thottappillil, V. A. Rakov, M. A. Uman, W. H. Beasley, M. J. Master, and D. V. Shelukhin, “Lightning subsequent-stroke electric field peak greater than the first stroke peak and multiple ground terminations,” *Journal of Geophysical Research: Atmospheres*, vol. 97, no. D7, pp. 7503–7509, May 1992, doi: 10.1029/92JD00557.

[18] R. B. Anderson and A. J. Eriksson, “The Measurement of Lightning and Thunderstorm Parameters Including the Application of Lightning Flash

Counters," in *Electrical Processes in Atmospheres*, Heidelberg: Steinkopff, 1976, pp. 724–727. doi: 10.1007/978-3-642-85294-7_116.

[19] D. R. MacGorman, M. W. Maier, and W. D. Rust, "Lightning strike density for the contiguous United States from thunderstorm duration records," United States, 1984. [Online]. Available: http://inis.iaea.org/search/search.aspx?orig_q=RN:16009891

[20] V. A. Rakov, R. Thottappillil, and M. A. Uman, "On the empirical formula of Willett et al. relating lightning return-stroke peak current and peak electric field," *Journal of Geophysical Research: Atmospheres*, vol. 97, no. D11, pp. 11527–11533, Jul. 1992, doi: 10.1029/92JD00720.

[21] M. A. Uman and D. K. McLain, "Magnetic field of lightning return stroke," *J Geophys Res*, vol. 74, no. 28, pp. 6899–6910, Dec. 1969, doi: 10.1029/JC074i028p06899.

[22] V. A. Rakov, "Lightning Return Stroke Speed," 2006. [Online]. Available: www.jolr.org

[23] Conseil international des grands réseaux électriques. Comité d'études C4. and Impr. Conformes), *Lightning parameters for engineering applications*. CIGRÉ, 2013.

[24] M. Hashmi, M. Lehtonen, and S. Hänninen, "Modelling and Analysis of Lightning Overvoltage Protection of MV Cable Laterals Connected with Overhead Lines," *Electronics and Electrical Engineering*, vol. 123, no. 7, Sep. 2012, doi: 10.5755/j01.eee.123.7.1325.

[25] N. Khadka, A. Bista, D. Bista, S. Sharma, and B. Adhikary, "Direct Lightning Impact Assessment on a Rural Mini-Grid of Nepal," in *2021 35th International Conference on Lightning Protection (ICLP) and XVI International Symposium on Lightning Protection (SIPDA)*, IEEE, Sep. 2021, pp. 1–7. doi: 10.1109/ICLPandSIPDA54065.2021.9627423.

[26] F. H. Silveira and S. Visacro, "On the Lightning-Induced Voltage Amplitude: First Versus Subsequent Negative Strokes," *IEEE Trans Electromagn Compat*, vol. 51, no. 3, pp. 741–747, Aug. 2009, doi: 10.1109/TEMC.2009.2025268.

[27] F. H. Silveira, A. De Conti, and S. Visacro, “Voltages Induced in Single-Phase Overhead Lines by First and Subsequent Negative Lightning Strokes: Influence of the Periodically Grounded Neutral Conductor and the Ground Resistivity,” *IEEE Trans Electromagn Compat*, vol. 53, no. 2, pp. 414–420, May 2011, doi: 10.1109/TEMC.2011.2106134.

[28] A. Piantini, A. Borghetti, and C. A. Nucci, “Lightning interaction with medium-voltage overhead power distribution systems,” in *Lightning Interaction with Power Systems - Volume 2: Applications*, Institution of Engineering and Technology, 2020, pp. 113–172. doi: 10.1049/PBPO172G_ch4.

[29] J. Zhang *et al.*, “Evaluation of the Lightning-Induced Voltages of Multiconductor Lines for Striking Cone-Shaped Mountain,” *IEEE Trans Electromagn Compat*, vol. 61, no. 5, pp. 1534–1542, Oct. 2019, doi: 10.1109/TEMC.2018.2869752.

[30] J. Zhang, Q. Zhang, F. Zhou, Y. Ma, H. Pan, and W. Hou, “Computation of Lightning-Induced Voltages for Striking Oblique Cone-Shaped Mountain by 3-D FDTD Method,” *IEEE Trans Electromagn Compat*, vol. 61, no. 5, pp. 1543–1551, Oct. 2019, doi: 10.1109/TEMC.2018.2869607.

[31] IEEE Power Engineering Society. Transmission and Distribution Committee., Institute of Electrical and Electronics Engineers., and IEEE Standards Board., *IEEE guide for improving the lightning performance of electric power overhead distribution lines*. Institute of Electrical and Electronics Engineers, 1997.

[32] S. P. da Silva, A. Piantini, J. L. Franco, and J. Gonçalves, “Lightning performance studies for a 13,8 kV distribution network,” in *International Symposium on Lightning Protection*, IEE/USP, 2003.

[33] M. Paolone, C. A. Nucci, E. Petrache, and F. Rachidi, “Mitigation of Lightning-Induced Overvoltages in Medium Voltage Distribution Lines by Means of Periodical Grounding of Shielding Wires and of Surge Arresters: Modeling and Experimental Validation,” *IEEE Transactions on Power Delivery*, vol. 19, no. 1, pp. 423–431, Jan. 2004, doi: 10.1109/TPWRD.2003.820196.

[34] S. Yokoyama, “26 th-30 th,” 2007.

[35] A. "Piantini and J. M. [Sao P. Univ. “Janiszewski SP (Brazil)],” “Use of surge arresters for protection of overhead lines against nearby lightning,” Institut de

Recherche d`Hydro-Quebec, Varennes, PQ (Canada), Canada, 1997. doi: https://doi.org/.

[36] J. Chen and M. Zhu, “Calculation of Lightning Flashover Rates of Overhead Distribution Lines Considering Direct and Indirect Strokes,” *IEEE Trans Electromagn Compat*, vol. 56, no. 3, pp. 668–674, Jun. 2014, doi: 10.1109/TEMC.2014.2309146.

[37] M. Hashmi, M. Lehtonen, and S. Hänninen, “Modelling and Analysis of Lightning Overvoltage Protection of MV Cable Laterals Connected with Overhead Lines,” *Electronics and Electrical Engineering*, vol. 123, no. 7, Sep. 2012, doi: 10.5755/j01.eee.123.7.1325.

[38] R. P. de S. Barradas, G. V. S. Rocha, J. R. S. Muniz, U. H. Bezerra, M. V. A. Nunes, and J. S. e Silva, “Methodology for Analysis of Electric Distribution Network Criticality Due to Direct Lightning Discharges,” *Energies (Basel)*, vol. 13, no. 7, p. 1580, Apr. 2020, doi: 10.3390/en13071580.

[39] F. Mahmood, M. E. M. Rizk, and M. Lehtonen, “Risk-based insulation coordination studies for protection of medium-voltage overhead lines against lightning-induced overvoltages,” *Electrical Engineering*, vol. 101, no. 2, pp. 311–320, Jun. 2019, doi: 10.1007/s00202-019-00783-z.

[40] S. Okabe, J. Takami, T. Tsuboi, G. Ueta, A. Ametani, and K. Hidaka, “Discussion on standard waveform in the lightning impulse voltage test,” *IEEE Transactions on Dielectrics and Electrical Insulation*, vol. 20, no. 1, pp. 147–156, Feb. 2013, doi: 10.1109/TDEI.2013.6451353.

[41] R. H. G. Tan and V. K. Ramachandaramurthy, “A Comprehensive Modeling and Simulation of Power Quality Disturbances Using MATLAB/SIMULINK,” in *Power Quality Issues in Distributed Generation*, InTech, 2015. doi: 10.5772/61209.

[42] C. Gomes and V. Cooray, “Concepts of lightning return stroke models,” *IEEE Trans Electromagn Compat*, vol. 42, no. 1, pp. 82–96, 2000, doi: 10.1109/15.831708.

[43] H. H., “Analytische Blitzstromfunktion zur LEMP-Berechnung,” *18th ICLP, Munich, Germany, 1985*, 1985, Accessed: Apr. 21, 2024. [Online]. Available: https://cir.nii.ac.jp/crid/1573387450708315648

[44] H. F., “Traveling current source model for LEMP calculation,” *Proc. 6th Int. Symp. EMC, Zurich, Switzerland, 1985*, pp. 157–162, 1985, Accessed: Apr. 21, 2024. [Online]. Available: https://cir.nii.ac.jp/crid/1571980076298162816

[45] G. Diendorfer and M. A. Uman, “An improved return stroke model with specified channel-base current,” *Journal of Geophysical Research: Atmospheres*, vol. 95, no. D9, pp. 13621–13644, Aug. 1990, doi: 10.1029/JD095iD09p13621.

[46] C. A. Nucci, G. Diendorfer, M. A. Uman, F. Rachidi, M. Ianoz, and C. Mazzetti, “Lightning return stroke current models with specified channel-base current: A review and comparison,” *Journal of Geophysical Research: Atmospheres*, vol. 95, no. D12, pp. 20395–20408, Nov. 1990, doi: 10.1029/JD095iD12p20395.

[47] J. Mahseredjian, “EMTP ® User Manual,” 2016. [Online]. Available: www.emtp.com

APPENDIX

- Surge Arrester circuit diagram

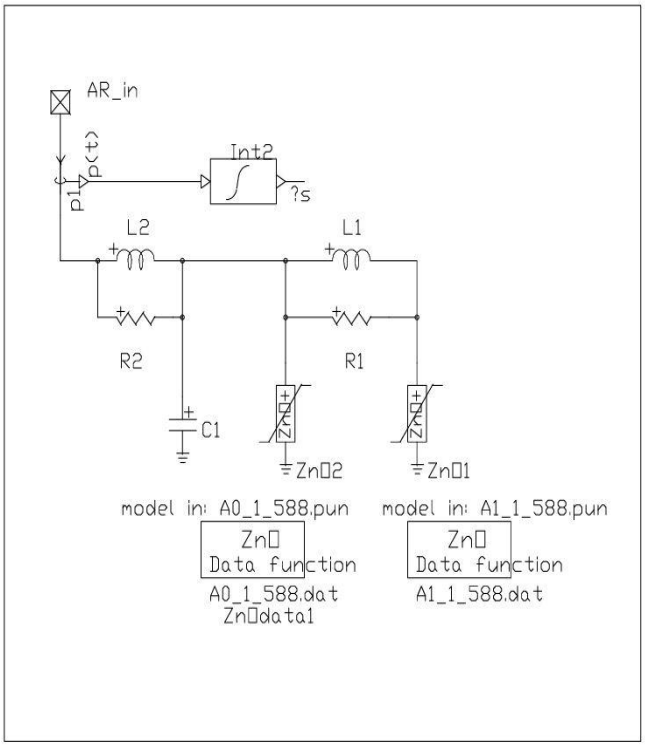

- CIGRE concave lightning current source

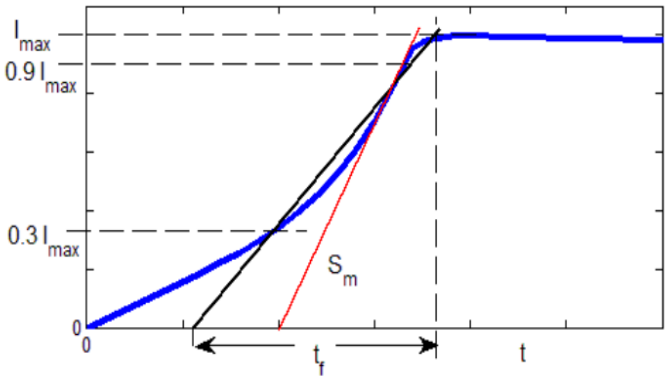

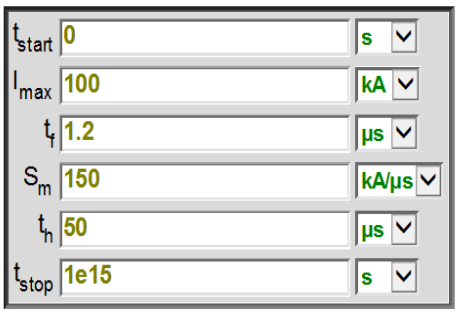

- Overall system circuit diagram

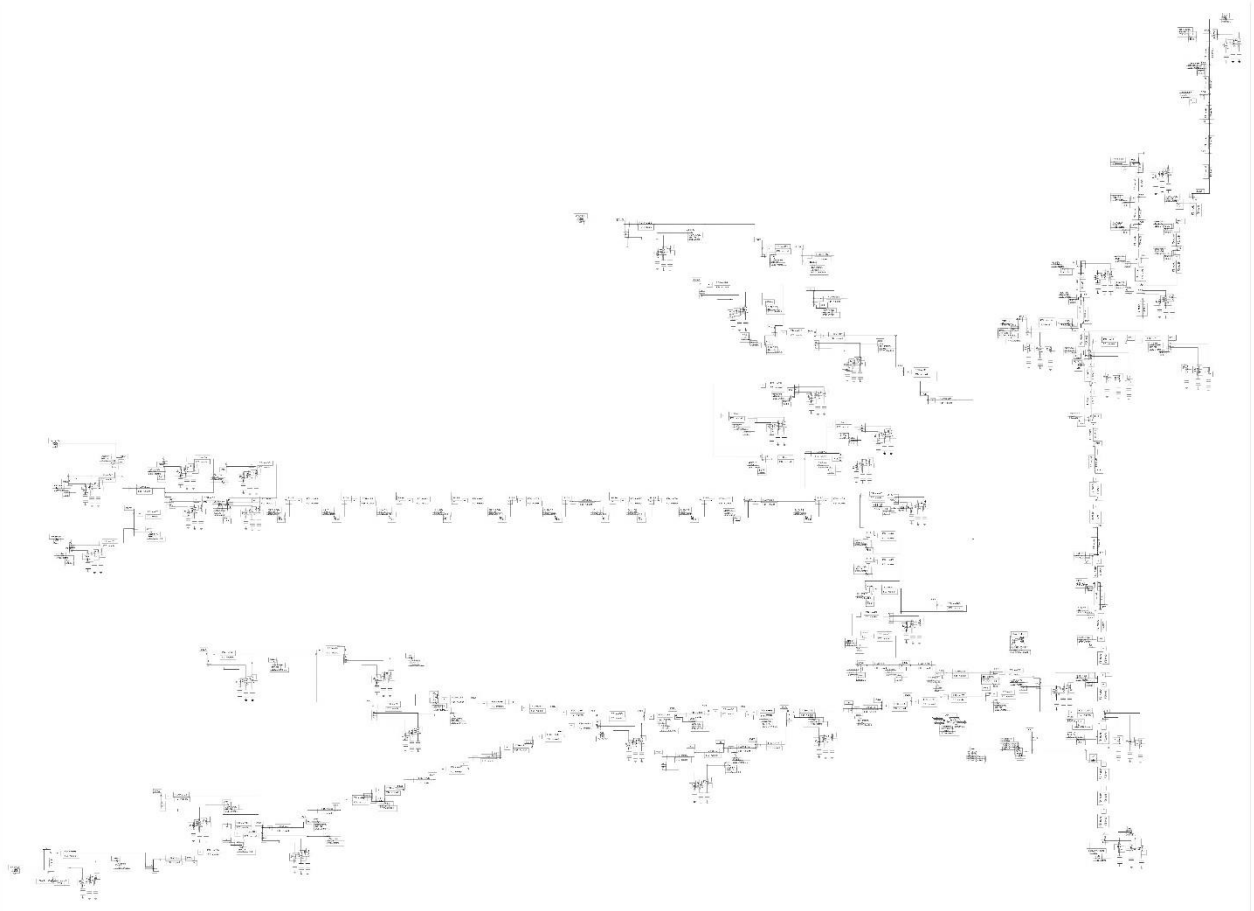

System Circuit Diagram in EMTP

Pulchowk Campus
Institute of Engineering
Tribhuvan University

ANUP DEVKOTA <078msree003.anup@pcampus.edu.np>

Direct Lightning Impact Assessment in Solar Mini Grid

2 messages

ANUP DEVKOTA <078msree003.anup@pcampus.edu.np> Mon, May 27, 2024 at 12:28 PM
To: jacem@acem.edu.np, premchandra.roy@acem.edu.np
Cc: basanta.gautam@pcampus.edu.np, laxman.motra@pcampus.edu.np

Dear Sir,
Please find the attached manuscript of my thesis work.

regards,
Anup Devkota
MSREE (2078)
9860023577

JACEM Anup Devkota.docx
407K

jacem advanced <jacem@acem.edu.np> Thu, Jun 6, 2024 at 5:55 PM
To: ANUP DEVKOTA <078msree003.anup@pcampus.edu.np>

Dear Author,

Your Journal Paper titled"
Direct Lightning Impact Assessment in Solar Mini Grid
"
has been accepted for the Journal of Advanced College of Engineering and Management (JACEM) for Vol.10, 2024. However, there are some minor changes that need to be done. Please look at the website for the format. We will contact you for further changes.

Regards,
Editorial Board

[Quoted text hidden]

Direct Lightning Impact Assessment in Solar Mini Grid

ORIGINALITY REPORT

17%
SIMILARITY INDEX

PRIMARY SOURCES

1	iclp2020.org Internet	182 words — 1%
2	hdl.handle.net Internet	106 words — 1%
3	Nasib Khadka, Diwakar Bista, Chandima Gomes, Shriram Sharma, Brijesh Adhikary. "Distribution Network Impact Assessment with Geometrically Identified Strike Points: An Approach", 2022 36th International Conference on Lightning Protection (ICLP), 2022 Crossref	85 words — 1%
4	Napolitano, F., A. Borghetti, C.A. Nucci, M.L.B. Martinez, G.P. Lopes, and G.J.G. Dos Santos. "Protection against lightning overvoltages in resonant grounded power distribution networks", Electric Power Systems Research, 2014. Crossref	81 words — 1%
5	mtc-m21c.sid.inpe.br Internet	73 words — 1%
6	vdocuments.site Internet	63 words — < 1%
7	www.scilit.net Internet	58 words — < 1%

8	Xiangpeng Fan, Wen Yao, Yang Zhang, Liangtao Xu et al. "Parametric Reconstruction Method for the Long Time-series Return-stroke Current of Triggered Lightning based on the Particle Swarm Optimization Algorithm", IEEE Access, 2020 Crossref	51 words — < 1%
9	www.emtp.com Internet	48 words — < 1%
10	kathmandupost.com Internet	47 words — < 1%
11	www.mdpi.com Internet	43 words — < 1%
12	Adonis F.R. Leal, Vladimir A. Rakov. "Processes in negative and positive CG lightning flashes detected from space by GLM", Electric Power Systems Research, 2024 Crossref	40 words — < 1%
13	diglib.tugraz.at Internet	39 words — < 1%
14	link.springer.com Internet	39 words — < 1%
15	Vahidi, Behrooz. "Non-Standard Lightning Overvoltages on Transmission Systems", The University of Manchester (United Kingdom), 2022 ProQuest	37 words — < 1%
16	elibrary.tucl.edu.np Internet	36 words — < 1%
17	res.mdpi.com	